International Research Journal of Engineering and Technology (IRJET) e-ISSN: 2395-0056
Volume: 06 Issue: 03 | Mar 2019 www.irjet.net p-ISSN: 2395-0072

HUMAN POWERED ORNITHOPTER

Mr. Kaushik Changmai,Mr. Md Akil Ahmed,Ms. Deborah Joseph

Final Year Students

Mr.A.Vivekananthan. Asst.Prof,Department Of Aeronautical Engineering,Excel Engineering College,Komarapalayam.

Abstract:*This paper proposes a concept of developing a flying vehicle with flapping wings that mimic the dragonfly flight mechanism which will be powered by the force of the pilot through pedals without the installation of any propulsive devices. The translatory and rotatory motion of the generated through the pedals will be transmitted to the wings using a gear mechanism which will provide the required lift and the propulsive force to the vehicle. The concept of this project will experiment on a miniature prototype which will adopt the flying mechanism of the dragonfly incorporated with a microprocessor. The rigid structure of the fuselage and the four wings will be designed using designing software such as the AUTOCAD and CATIA and the fabrication of the design will be done using rapid prototype. From this prototype, the thrust, lift generation, and possible weight limit will be evaluated from analysis software ANSYS as well as physical true values, and the performance characteristics, as well as the flight attitude, will be analyzed too. Hopefully, if the prototype shows the positive performance characteristics, the upscale of the full-fledged flying vehicles model powered by the pilot with the mimic of dragonfly flight mechanism will be designed and developed further. This project was started off with an objective to design and develop an autonomous flying vehicle mimicking the flapping motions of tiny insects and birds, especially in this project dragonfly is chosen, without installation of any kind of the propulsive devices such as engine which will be able to help in developing low noise signature surveillance aircraft, pollution-free flying vehicles and transportation and provide aid to the disaster management services.*

Keywords: **Ornithopter, flapping-wings, dragonfly flight-mechanism, autonomous flying vehicle.**

INTRODUCTION

1.1 Background

1.1.1 The motivation for Insect based Ornithopters

Over 99.9 % of the 900,000 species of insects in the world are classified as Pterygota or winged insects. Michael Dickinson, an entomologist at the University of California at Berkeley says, “Insects don’t just stay in the air, they perform aerial maneuvers, fly up, down and sideways, and respond to changes in wind speed and direction.” Even though they are characterized as one of the tiniest living things with the ability to fly, their flight mechanism has been a huge challenge for scientists and researchers to understand until recently. Some insects fly breaking the rules of aerodynamics such as the bumblebee,

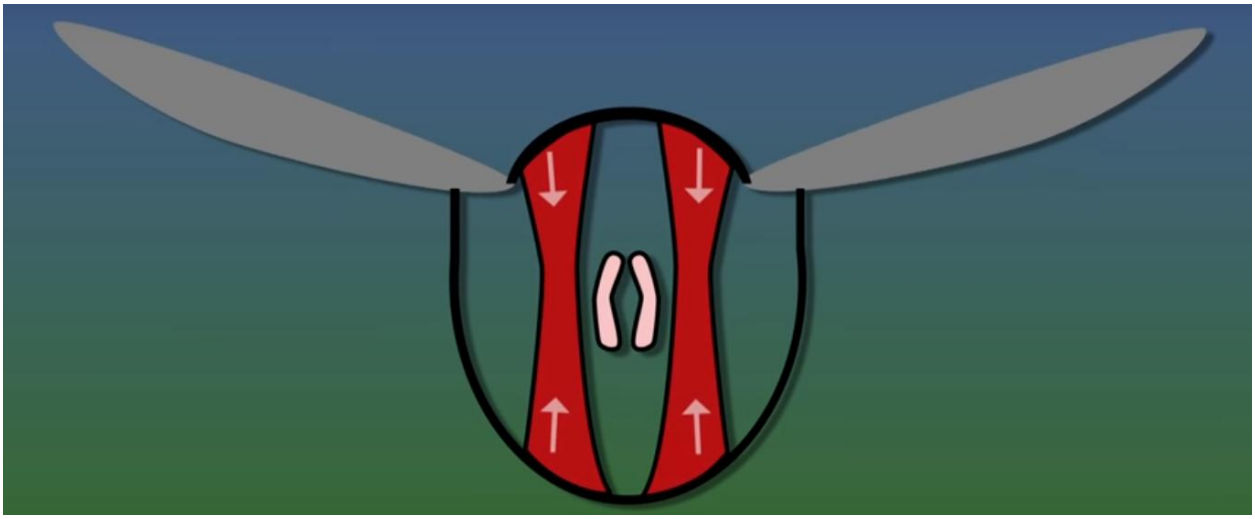

Fig 1.1 Indirect Musculature in Advanced Flying Insects

these facts are capturing to learn more about the mechanism involved in the flight of these tiny insects that almost rule the world of the flying creatures. In the near past, many miniature UAVs have been designed drawing inspiration from these very efficient insects. The flight mechanism of insects is broadly classified as direct and indirect musculature flight.

In advanced flying insects, both the up-stroke and down-stroke are produced by indirect muscles through the distortion of the thoracic cuticle. The insect asynchronous flight muscles have the property of being stretch-activated i.e. when they stretch, they contract. When the pivot point of the wing is pulled down, it gives the up-stoke and when it is pushed up it gives the down-stroke.

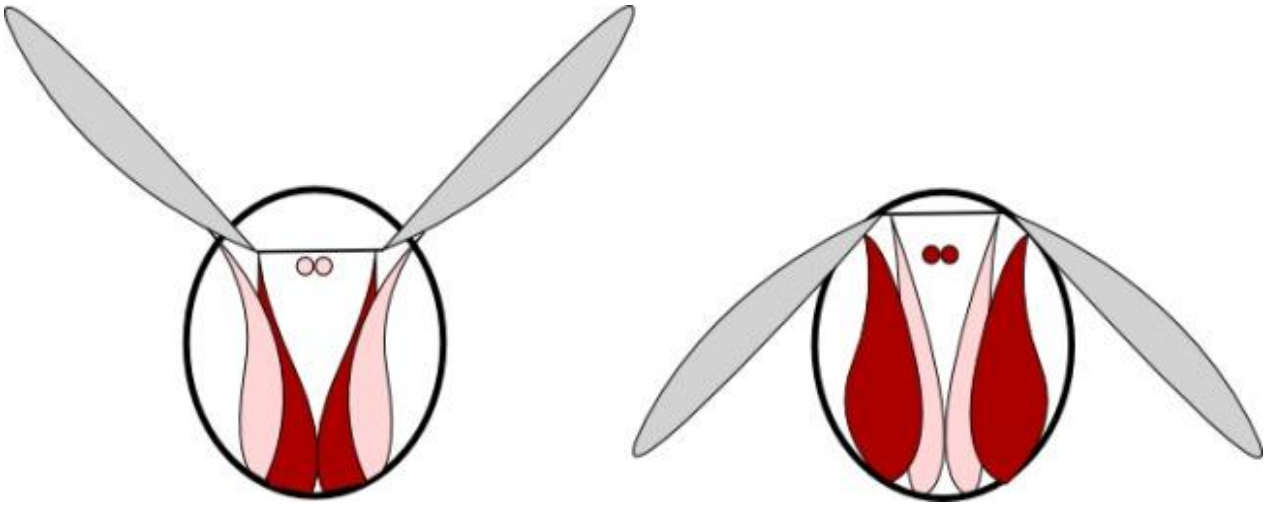

Fig 1.2 Direct Musculature

The muscle that causes the up-stroke are called the vertical muscles, when these muscles contract or shorten then two actions occur simultaneously; one, these muscles bulge out and they pull down on the wing causing the up-stroke. When these muscles are shortened, they stop contracting and this bulges the body of the insect. The other set of muscles are called the horizontal muscles that run the length of the body of the insect.

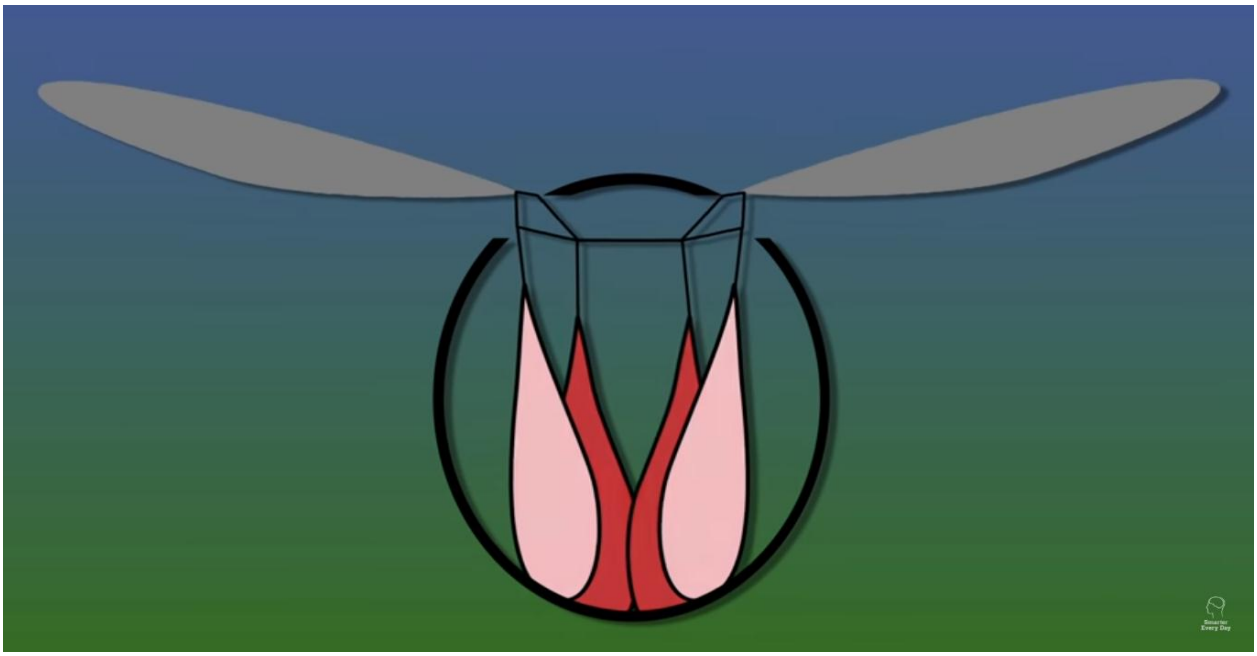

Fig 1.3 Direct Musculature in dragonflies

When these muscles are shortened, they stop contracting and this bulges the body of the insect. The other set of muscles are called the horizontal muscles that run the length of the body of the insect. When these muscles contract or shorten they cause the horizontal body of the insect to shorten or bulge out which causes the top part of the insect body to push up. This upward movement not only pushes the top of the body up but also the base of the wings. This movement causes the wings to have a down-stroke. When the vertical muscles contract they generate the up-stroke and when these relax, the horizontal muscles contract to generate the down-stroke. This is how indirect musculature works.

The most primitive flying insects are dragonfly, damselfly, and mayfly and they have what is called, '*Direct Musculature'* or *'Direct Flight Muscles'* while the advanced flying insects possess *'Indirect Flight Muscles.'* In both these cases, Indirect Dorso-Ventral Muscles produce the up-stroke but in the primitive orders, muscles are attached directly to the base of the wing to produce the down-stroke. In the case of a dragonfly, the muscles are directly attached to the wings and each movement of the wing is caused by the corresponding movement in the muscles. Their muscles pull directly on the wing and are able to operate each wing independently in both directions. This is why they dominate the insect flying world. The front and hind wings move independently and there is a phase difference in the movement of the two pairs, i.e., when one pair is moving up the other pair is moving down. This gives 20% more efficiency in flight compared to just two wings. Dragonfly wings have a spot named Pterostigma on the leading edge of the wing which is actually heavier than the rest of the wing. This complex aerodynamic structure is built right into the wing of a dragonfly to help hem glide. Similarly, all the flying insects have some detailed difference from each other in the motion of flight. This diversity in the flying world is interesting and challenging to learn more about. Thus for this project, we decided to lay our entire focus on studying and understating the flight mechanisms of the most common insects that we almost see every single and to adopt the most efficient of it all to mimic for the flight mechanism of the human-powered ornithopter.

1.1.2 Reason For Opting Dragonfly Flight Mechanism

In the flying world, the dragonflies are considered as the primitive insects but their flight system is nothing less than wonder that took scientists and researchers ages to unravel. They are most commonly known for being the inspiration behind the idea of the first helicopters ever manufactured, but there is more to dragonflies than just their unrivaled ability to hover for a prolonged period of time. Dragonflies are titled as the "masters of air" for their of the flight. They can fly up, down, forward and even backward. Each wing of a dragonfly has its own muscles permitting each individual wing to alter its stroke frequency, amplitude, phase, and angle of attack. The front wings beat down while the rear ones make an upbeat. The wings can lock horizontally this aids the dragonflies use to glide or rest while in the air. The wings of dragonflies blend flexibility and strength flawlessly together. The arbitrary shapes in the wings serve varied purposes such as, the hexagonal shapes flying skills that are not only very different from the other insects but also extremely impressive and inspiring. Physically what sets them apart is the possession of four wings instead of the conventional two wings like their other flying counterparts do. These wings allow them to perform various flight maneuvers and hover at the same time. They own the ability to accelerate in any direction at any time are the flexible parts that are most likely do the part of bending and swaying; while the quadrilaterals are the rigid and strong parts of the wing that does not move much but stays rather stable during the flight. The tips of the wings possess stabilizers like structures that benefit its flight.

Jane Wang, a lead researcher of "*The Secret of Dragonflies' Flight*" stated, "The wings on an airplane are oriented at some fixed angles. But insects have the freedom to rotate their wings and by adjusting wing orientation, dragonflies can change the aerodynamic forces acting on each of their four

Fig 1.4 Hind wings of a dragonfly

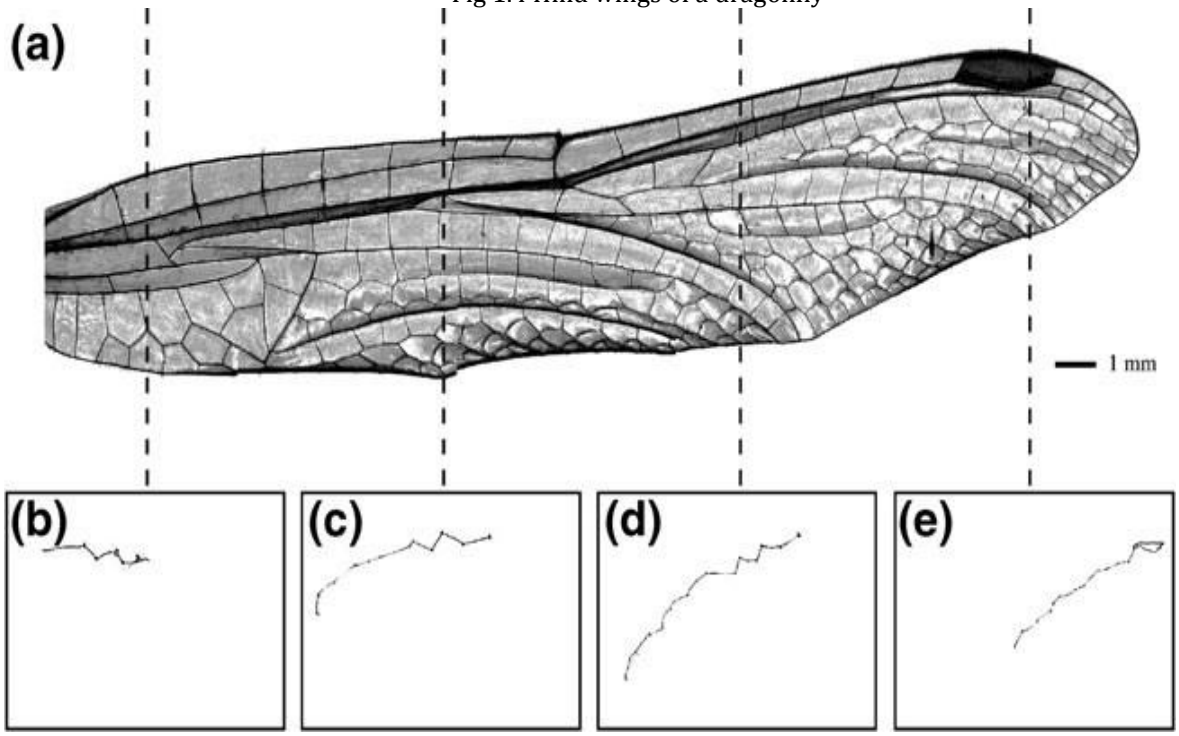

wings." From the tests and studies conducted it was learned that dragonflies can adjust the stroke plane (the direction in which they flap their wings) orientation of each wing independently.

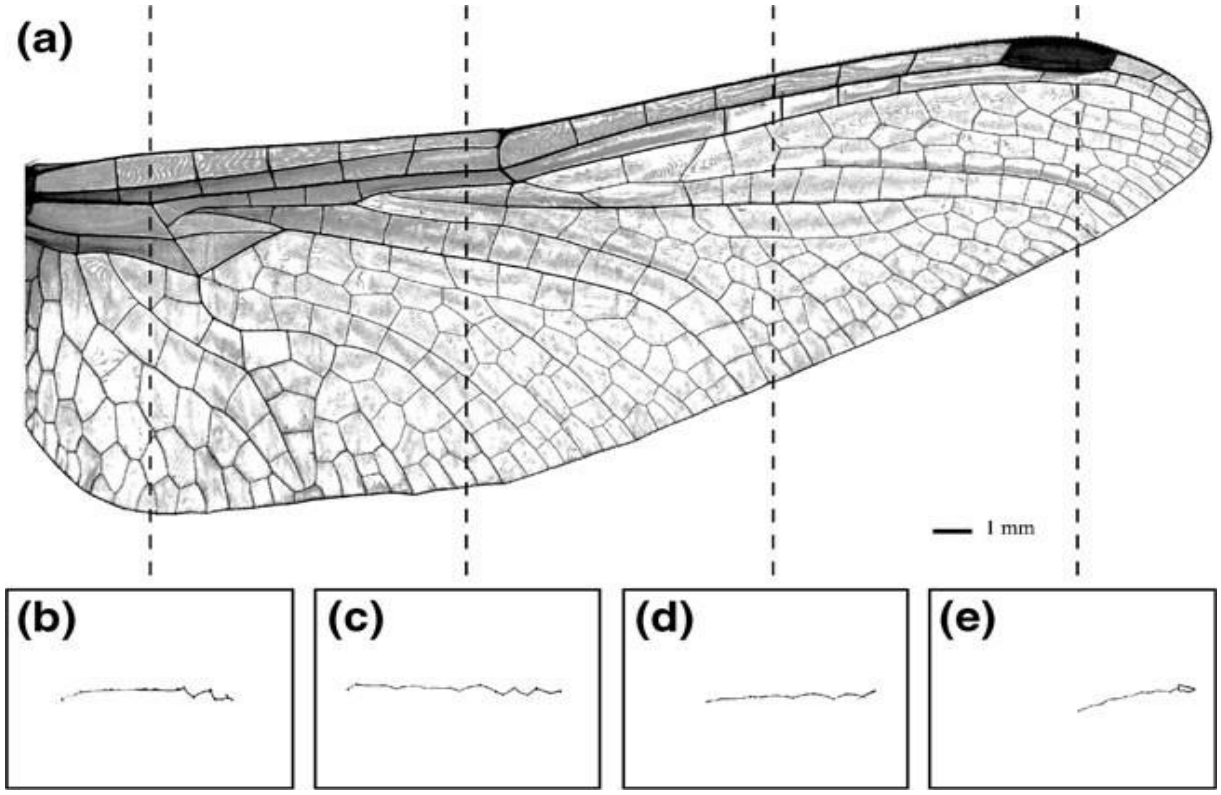

Fig 1.5 Fore wings of a dragonfly

Unlike other flying creatures, dragonflies do not try to overcome drag; instead, they actually use drag to stay aloft. The asymmetrical flapping of its wings causes the down stroke to create drag which supports the weight of the dragonfly. When the sings beat out of phase, the rear wing creates an induced flow that reduces the drag on the front wings. The flapping of their wings creates tiny whirlwinds under them. Dragonfly wings are highly corrugated, which increases the stiffness and strength of the wing significantly, and results in a lightweight structure with good aerodynamic performance. The inertial loads are 1.5 to 3 times higher than aerodynamic pressure loads. Further, it is found that wing deformation is smaller during the downstroke than during the upstroke, due to structural asymmetry. The natural vibration mode analysis revealed that the structural natural frequency of a dragonfly wing in a vacuum is 154 Hz, which is approximately 4.8 times higher than the natural flapping frequency of dragonflies in hovering flight (32.3 Hz). This insight in the structural properties of dragonfly wings could inspire the design of more effective wings for insect-sized flapping micro air vehicles: The passive shape of aero-elastically tailored wings inspired by dragonflies can in principle be designed more precisely compared to sail like wings which can make the dragonfly-like wings more aerodynamically effective. The maximum aerodynamic load at mid-stroke and the maximum inertial load at stroke reversal, these loads are summed along the chord to obtain a spanwise distribution along the wing. The distributions are similarly shaped from root to tip, with local maxima for the inertial load at the nodes (±45% wing length) and pterostigma (±85%). The maximum aerodynamic load is found at about 65% of the wingspan. The inertial forces along the wingspan are approximately 1.5–3 times higher than the aerodynamic forces. Bending moments due to the inertia of flapping wings are about twice as large as those due to aerodynamic forces. The simultaneously plotted mass distribution shows that local spanwise mass maxima appear at the wing nodes and the pterostigma. The peaks suggest that these areas have a relatively large influence on inertial deformation responses. The wing's angular and translational velocity is zero during stroke reversal; aerodynamic loads are therefore not present.

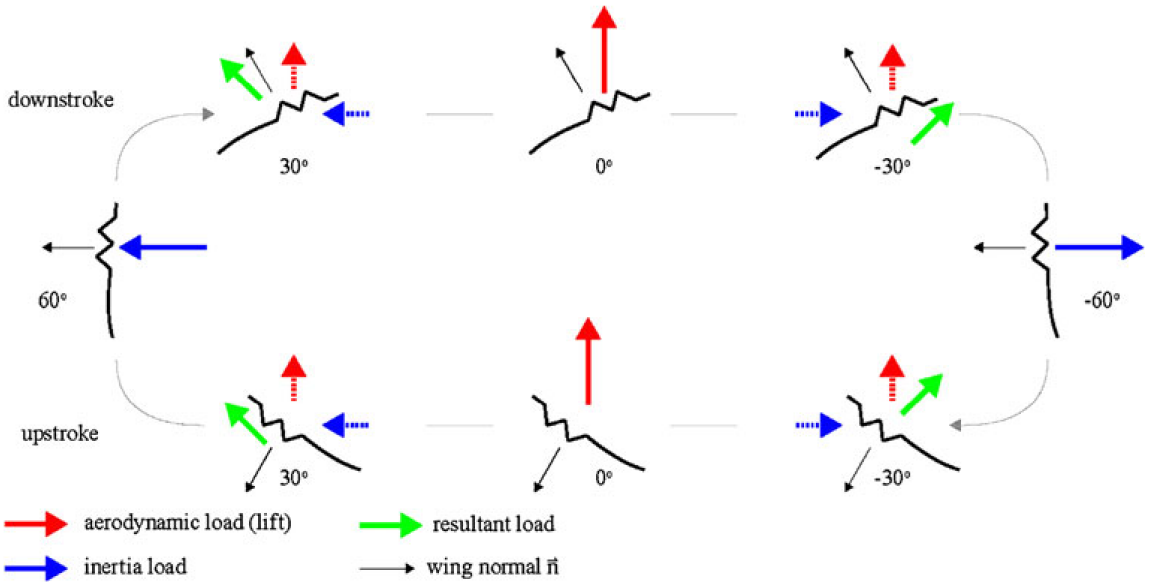

Figure 1.6 The flapping movements of a dragonfly's wings

1.2 Inspiration for Ornithopter

1.2.1 Concept of Ornithopters

An ornithopter is a name given to flying vehicle (aircraft) that flies by flapping its wings. Its thrust and lift are derived from the mechanism of flapping the wings. Ornithopters imitate the flying creatures of nature as none of them having rotating parts. The principle of operation of the ornithopter is same as the airplane; the forward's motion through the air allows the wings to deflect air downwards, producing lift. The flapping motion of the wings takes the place of a rotating propeller. Theoretically, the flapping wing can set to zero angles of attack on the upstroke, so it passes easily through the air. Since typically the flapping airfoils produce both lift and thrust, drag-inducing structures are minimized. Use of flapping wings offers even larger displaced air mass, moved at lower velocity, thus proving efficiency. Birds and insects do not fly by means of a simple up and down flapping motion of the wings; instead, they use several subtle mechanisms that modify the vertical flapping motion. The wingtip strokes of larger birds follow simple patterns like ovals or figures of eights. Flapping wing aerodynamics is characterized by unsteady aerodynamics. According to a paper n "*Effect of Different Design Parameters on Lift, Thrust and Drag of an Ornithopter"* by M Afzal Malik and Farooq Ahmad, the flapping wings can have three distinct motions with respect to three axes as a) Flapping- which is up and down plunging motion of the wing. Flapping produces the majority of the bird's power and has the largest degree of freedom. b) Feathering- is the pitching motion of the wing and can vary along the span. c) Lead-lag, which is in-plane lateral movement of the wing.

The essential parts of an Ornithopter as listed by a paper on *"Ornithopter Design and Development"* are: (A) Gear Box- gear mechanisms are used to provide sufficient torque to flap the wings. Two or more gears working in tandem are called a transmission and can produce a mechanical advantage through a gear ratio and thus may be considered a simple machine. Geared devices can change the speed, magnitude, and direction of a power source. (B) Main Body- Basically to reduce the overall weight of the ornithopter, the main body is made of lightweight materials such as Balsa Wood or Carbon. A proper mount is attached in front of the body frame for motor and gearbox. (C) Wing- For an ornithopter to be effective and efficient, it should be capable to flap its wings to generate

enough power to get off the ground and travel through the air. The efficient flapping of the wing is characterized by pitching angles, lagging plunging displacements by approximately 90 degrees. To increase the efficiency of the ornithopter, more power is required on the downstroke than on the upstroke. If the wings of the ornithopter are not flexible and flapped at the same angle while moving up and down, the ornithopter will act like a huge board moving in two dimensions, not producing lift or thrust. The flexibility and movability of the wings enable their twist and bend to the reactions of the ornithopter while in flight. (D) Tail Wing- In order to steer an ornithopter efficiently and perform turns easily, a necessary condition is the stabilization of a fee flight ornithopter, which depends on its tails. The tail of an ornithopter is generally a V-shaped tail with an angle of 120 degrees. Two steppers or servos are mounted on the body frame to move the rudders attached to the tail, which are used to change the direction and pitch of the ornithopter. The wings of the ornithopter are attached to the body at a slight angle, which is called the angle of attack; the downward stroke of the wing deflects air downward and backward, generating the lift and thrust. The surface of the wings is designed flexible which causes the wings to flex to the required angle of attack in order to produce the forces essential for achieving flight.

1.2.2 History of the Concept of Ornithopters

Since the beginning of times, every creature that flew has been a source of fascination for human beings and the freedom of flight has always been more than just a desire. Be the poets, the scholars, the scientists or any professional, the thought of escaping the inevitable force of gravity and fly free in the air even for a fleeting moment has been penned down over the ages. For years man has attempted to replicate the flight of the bird looking to nature's design. With the increase in development, science gradually shifted to the concept of balloons and fixed win flights but even now the freedom and effortless grace of birds are as captivating as ever. Records of attempts to fly date back as early as A.D 60, perhaps the first attempt to be met with some success was that of Eilmer, a Benedictine monk who was seriously injured after gliding about 200 yards from the tower of Malmesbury Abbey in 1060. Various unsuccessful attempts were made later on in history. Leonardo Da Vinci sketched in his notebook a device designed to be powered by man, what set his idea apart from his predecessors was the fact that instead of simply strapping a set of wings to a man's arms, his idea called for a machine that would carry a man while harnessing his power.

Otto Lilienthal, popularly known for his glider experiments was also keenly interested in designing ornithopters. His ultimate desire was to produce a manned, engine-powered flying machine. Lilienthal's ornithopter design was to have been powered by a single cylinder engine driving the flapping motion of the outer portion of each wing. He patented the machine in 1893, and despite repeated failures of the carbonic engine he intended to use for power, Lilienthal began building a second ornithopter, this time with a new engine and a larger frame. Despite his careful observations, lacked the tools to fully understand the mechanics of a bird's wings; and further scientific analysis in an aerodynamic sense would not come for nearly four decades. An accurate understanding of how a bird is able to achieve forward thrust by way of flapping its wings was not gained until the early 1900s, when Knoller, in 1909, and Betz, in 1912, partnered to explain the phenomenon that had for so long escaped comprehension of human aeronauts. Working independently, Knoller and Betz were the first to observe that a flapping wing creates an effective angle of attack, and in doing so generates a normal force vector of both lift and thrust components. Although widespread experimentation with ornithopters as a means of achieving manned flight largely faded after the Wright brothers' successful flight at the turn of the twentieth century, it never died out altogether. Many of the resulting efforts by those marginalized proponents of flapping wing flight were ill-fated, unscientific trials. A few stalwart visionaries, however, continued to work toward successful flapping wing flight, both human and engine powered and made substantial contributions to the development of the ornithopter.

1.2.3 The inspiration for Human Powered Ornithopters

Leonardo Da Vinci was also the first ever to suggest a human-powered ornithopter. His variety of ornithopter designs called for a pilot either prone or standing and operating the flapping wings by alternatively pushing or pulling on several levers. In each of his sketches, the pilot was to provide the motive power by which the machine would achieve lift as well as propulsive energy. His designs even included a transmission of sorts to convert a rowing motion into a vertical flapping movement. He was captivated by the longing to fly as birds do, saying: "With each advent of spring when the air is alive with innumerable happy creatures- then a certain desire takes possession of man. He longs to soar upward and to glide, free as the bird, over smiling fields, leafy woods, and mirror-like lakes, and so enjoy the varying landscape as fully as only a bird can do. The observation of nature constantly revives the conviction that flight cannot and will not be denied to man forever." After the successful Balloon flight, many attempts were made in Western Europe to fly human-powered ornithopter in the first half of the 19th century. By mid-century, ornithopter design had become significantly more complex but not more successful. Another pioneer in the context of human-powered ornithopter is Alexander Lippisch. Lippisch and Brustmann together developed a plan to produce a human-powered aircraft. They later settled on an ornithopter because of the potential benefit the design provided in terms of efficiency and weight. Although their ornithopter achieved what may be considered remarkable success, with the pilot, Hans Werner Krause maintaining a powered glide for over 300 meters on one of his final flights, the results of the tests were never published. 90 years later reflecting on his work, Lippisch remarked, "Today I am still inclined to think that wing flapping actually gives better efficiency, but our knowledge of how to design a highly efficient flapping wing is very limited." Almost a decade down the line, a young aircraft designer named Adalbert Schmid designed and built his own human-powered ornithopter. In 1942, Schmid's flapping wing aircraft reportedly flew over 900 meters under human power while maintaining its height above the ground.

LITERATURE REVIEW

2.1 Introduction

Since the early historic, humans obsessed with escaping gravity's unblinking gaze to somehow slip aloft sharing a universal desire for the freedom of flight even for a fleeting moment. This can be seen in anyways inspiring to poetic about the dream of flight. Looking to nature design, human for years attempted to replicate the flight of the birds and insects in many a bid to break free of his earthly bond. Human's dream of launched himself skyward to advance design, flapping wing crafts, known generally as ornithopters, have held a confine placed to achieved the freedom of fleeting aloft. In the past few decades, aircraft that capitalize on the flight mechanism of bird enjoyed a renaissance of sorts. From the Human-powered ornithopter flight to Nano-scale unmanned vehicles incorporated with flapping wing design has become an industrial scientific domain. This paper Includes the summarize literature for the several journals that have been published in the past few decades in the field of Ornithopter.

Muhammad Ridhawanbin Jumat[1][2014] design, built, and fly the University of Glasgow Singapore flapping wing Micro Aerial Vehicles using fabrication methods such as the laser cutting and prototyping. Using Laser cutting his first prototype made from the acrylic and the Ripstop. His second and third prototype was designed and fabricated using a 3D laser cutting technique. The flapping wing has multiple advantages compared to other types of MAVs as they can hover without making much noise. Flapping MAVs are resemblance either a bird or an insect. MAV can provide real-time intelligence during missions. They create a CAD design using SolidWorks of the dual gear crank and horizontal tail design. With one of a feature of the SolidWorks, they measured the total weight of the MAVs. Later on, for weight reduction, they chose a simple tilting tail. When they tested the MAVs, they find that increasing the RPM of the motor pitches the MAVs upward and decreasing on downwards. However, decreasing rpm too much would make the MAVs stall on landing. Despite the limitation of its melting points and breaking strength, Rapid Prototyping

Machine or the 3D printing is better for fabrication method than other methods.

*Jared Grauer [2][2010]*In several Sector of the Society, as the demands of the Miniature unmanned aircraft increase, flapping wing aircraft becomes one of the main domain, his work presented a complete nonlinear multibody model of the ornithopter flight dynamics guide by the flight test and system identification result and cast into a canonical form for nonlinear control. Obtaining an accurate model of flight dynamics for autopilot and autonomous operation is a challenging task. Jared and James paper present the development of a relatively low dimensional state of space model describing the ornithopter flight dynamics.

Mohd Firdaus Bin Abas[3][2016] Paper reviewed the kinematics, membranes, and flapping mechanisms ranges from small birds to big insects, which reside within the transition and the Low Reynold's number and the possibility of the applying piezoelectric transmission to produce NAV flapping wing motion and was mounted on the MAV instead of the motorized flapping wing transmission. They conducted a review of the flapping wing MAVs on both the flapping wing insects and ornithopter, and systematically summarize the contribution of the ornithopter and insect type flapping wing kinematics and membranes wing structures. In his paper, they recommended to the researcher on the development of MAV to consider adopting piezoelectric transmission system instead of the motorized transmission system as it would reduce the weight of the MAV significantly giving more space allowing to installed high definition cameras and sensors.

*Richard J. Bomphrey [4][2016]*work is a synthesis of the mechanics, aerodynamics and visually mediated control of the dragonfly and damselfly flight with the addition of the new experimental and computation data's in several key areas. Using extensive suite of the equipment's and the methodologies including specialize wind tunnel, two free flight arenas, high speed stereo-photogrammetry, a customized motion capture system and PIV Apparatus, they have identified that the structural corrugations do not significantly impact the aerodynamic impact of the dragonfly wings and natural corrugation can help to smooth stall characteristics at high angles of attacks.

Yanghai Nan[5][2018] paper represented geometric similarity and comprehensive scaling law in wing performance estimation through statistical analysis. His works show the ranges of the wing performance of the lumped mass parameter and the ratio of the flapping wing MAVs. His results provide a simple but powerful guideline for the design of flapping wing MAVs and the morphology of the natural flyers. The lumped parameter had comprehensively studied and observed the relationship between the lumped parameter and the aspect ratios, the lumped parameter is inversely proportional, and the lumped parameter is independent of the body mass through geometric similarity analysis. Then they defined the P_W –AR ratio and estimate the wing performance and aerodynamic performance.

*Shiva Prasad Uppu [6][2018]*work is to determine the aerodynamic properties of the dragonfly airfoils in comparison to the traditional smooth NACA 2.5411 airfoils. At low speed, simplified dragonfly airfoils are analyzed and a 3D printed model is tested using the Six Component Strain Gauge and compared the result with the NACA 2.5411 airfoils. At Low Reynold's number, Aerodynamic performance is evaluated with the regular section. Both the Experimental and numerical work was Carried out Over the models at different wind speed. His Result shows a completely nonlinear behavior resulting in positive Aerodynamic forces. With his work, they resulted that Dragonfly airfoils have better Aerodynamic characteristics like high C_l and C_l/C_d. due to Corrugated Cross-section, Dragonfly airfoils has more C_d when compared to NACA 2.5411 but in return, it offers more lift due to its vortices generated at the valley in the cross section and more lift generated when operated at the AOA.

*Jae Hyung Jang [7][2018]*paper proposed a wing root control mechanism inspired by the drag –based-system of the dragonfly to control the angle of the attack. They designed a spatial four-bar linked based flapping mechanism using a 3D printer. In the aerodynamic analysis, when the wing root angle of 0^o with the increased angle of attack of 30^o, the drag based system reduced the amplitude of the force in the horizontal direction to approximately 0.15N and 0.1N in the downstroke and upstroke respectively in compared with lift based system. The measured forced showed that MAV with wing rotation mechanism flies more stable when hovering and with changing the wing root angle, the flight mode can be changed easily.

Structural Analysis of a Dragonfly Wing(S.R. Jongerius & D. Lentink – 2010)

S.R Jongerius [8][2010] shows resonant frequency of the flapping wing is tuned for carrying the aerodynamic and

inertial load but they are not fully understood. His paper presented his work on the structural analysis of the dragonfly wing. They create a 3D scan of a dragonfly with a micro CT-scanner, which contains complete venation patterns including thickness variation throughout, and approximated the forewing architecture with efficient 3D Beam and shell and then determined the wing deformation and wings natural variation modes. As a result, from his computation, because of the structural asymmetric, deformation is larger in upstroke than downstroke. Also, found that, at vacuum, the natural frequency of dragonfly is 154 Hz and in Hovering flight 32.3 Hz. Thus, these structural properties and his aero elastically tailored wings of dragonflies inspire to design of more effective wings for MAVs and NAVs.

Yu Chong Tai [9][2010] developed the first electrically powered palm size ornithopter was flown for 9 seconds in October 1998, which powered by two 1- farad super capacitor as his first prototypes. The second prototype houses a small 3-gram rechargeable NI-Cad Battery and the best performance lasted 22 seconds. Moreover, they studied the flapping wing flight in the wind tunnel using wings developed by MEMS technology.

The conventional way to construct the wing is to build the wing spars and its membranes from the light yet very strong materials. They first built the model using Carbon fiber rod with 750mm diameter as wing frames. Thin Mylar or thin paper glued to the carbon rods as the wing membranes. This method of constructing the wing is cumbersome and need to consider:

1) Glue adds weight and wing becomes too heavy
2) An identical set of wings are difficult to achieve unless molds are made for each fabrication
3) It is costly,time-consuming and has low turnaround time.

MEMS wing enables systematic research in term of repeatability, size control, weight minimization, mass production and fast turnaround time, in addition to this, a complicated structure such as dragonfly, butterfly, and beetles wing can be easily fabricated using photolithography technology. They have chosen the titanium alloy (Ti-6A1-4V) because of it's lightweight, strong and can easily taper to vary the thickness of wing pars and titanium alloy is ductile allowing bending to create wing camber to improve performance. For wing membrane parylene - C,as

1. It can be deposited directly onto titanium alloy at any desired thickness
2. Its adhesion to titanium- alloy isexcellent
3. It is light and strong and can withstand high flapping frequency of more than 30 hertz without
4. It is a deposit at room temperature and yields a conformal coating. Based on simplicity, minimal weight, flapping symmetry, the design of C was implemented and built with a small DC motor with gearbox ratio of 22:1, which used to drive the transmission, which powered by 1.5 watts. The Wings ware mounted on the transmission system and several flapping tests were performed and can withstand more than 30 hertz of flapping without breaking ortearing.

A high-quality low-speed wind tunnel with velocity uniformity of 0.5% and speed from 1m/s to 10m/s was operate taken using the low capacity 2-D force load cells.

His result provides the following statements:

1. The spanwise stiffness is an important factor in lift production in flapping wing
2. The leading edge produce larger lift coefficient compared to those with flexible lading edges
3. At the start of the downstroke, the flow stagnates at the leading edge of the wing.
4. The stagnation line progressively moves to the upper surface of the wing thereby forming a leading-edge vortex which continues to grow and its maximum size at about the middle of the downstroke and then starts the upstroke.
5. Because of light and rigid nature, the real wing shows better wind tunnel test result than nature mimics Mems wings.
6. The latest Microbat prototype was designed with battery powered with a radio control system which flown on 7 December 2000 for 42 seconds on its first flight.

The key to the time limit of flight is due to the power sources, which remains an impotent issue.

*Benjamin J. Goodheart [10][2011]*Aviation historians as "tower jumpers" often refer to the earliest of those to experiment

with flapping wing devices. In keeping with his titles, these aspiring aviators typically followed the approach of the mythical Daedalus, often building a set of wings from actual feathers. Thought the records of an attempt to fly in this manner exist as early as A.D 60.

Eilmer, a Benedictine monk, who was seriously injured after gliding about 200 yards from the tower of Malmesbury Abbey in 1060. Many years later, the arts of flight had not advanced appreciably, as, in 1742, the Marquis de Bacqueville met with a fate similar to his monastic predecessor when he too leaped from tower to fly across the river scene. As early as thirteen century, the scientifically incline Franciscan monk Roger Bacon suggested a flying machine that was propelled by "artificial wings to beat the air "offering what is like the first record of an ornithopter.

Around 1486, Leonardo da Vinci, the Florentine scientist, and painter sketched in his notebook a device designed to be power by man. Da Vinci's ideas set him apart from his predecessor in that, rather than simply strapping set wings to man's arms, they called for a machine that would carry a man while harnessing his power. His design includes a transmission of sorts to convert a rowing motion into vertical flapping motion.

Sir George Cayley's research led him to believe that many experiments that have been pursuing flight in ways unsupported by science. Writing on the subject Cayley issued the following prophetic word that was to predict the future of aviation and signal the eventual demise of the ornithopter and especially the human-powered ornithopter as the primary design on which to model:

The idea of attaching wings to the arms of a man is ridiculous enough, as the pectoral muscles of a bird occupy more than two third of its whole muscular strength, whereas in man, the muscle that could operate upon the wings thus attached, would probably not exceed one-tenth of the whole mass. There is no proof that weight for weight of a man is comparatively weaker than a bird, it is therefore probable if he can make to exert his whole strength advantageously upon a light surface similarly proportioned to his weight as that of the wing to the bird that he would fly like a bird. I feel perfectly confident, however, that is noble art will soon bring home to man's general convenience, and we shall be able to transport ourselves and our families, and his goods and chattels, more securely by air than water and with a velocity of from 20 to 100 miles per hours. To produce this effect it is only necessary to have a first mover, which will generate more power in a given time, in proportion to its weight than the animal system of muscles. (Gibbs-Smith, 1962, page 213-214)

In Da Vinci's many manuscripts, he gives one of the first written accounts of the manner in which birds describe a circular path in flight by changing the geometry of his wing. Da Vinci wrote at length concerning the use of the birds tail as a means of achieving stability as arresting speed and descent in flight. Da Vinci said 'a bird is an instrument working according to the mathematical law, which instrument it is within the capacity of the man to reproduce with all its movement.

Knoller and Bentz were the first to observe that a flapping wing creates an effective angle of attack and doing so generate a normal force vector of both lift and thrust components. Researcher, Katzymer confirm his theory and identify the actual condition under which a flapping airfoil generate thrust.

Since Alphonse Penaud's 1874 ornithopter model in which the wing was designed with a single covering attached only at the leading edge, with stiffening ribs extending chordwise, most flapping wing designs have been constructed similarly.

DeLaurier has not only unlocked many old mysteries of mechanical emulation of bird flight, but he also provides the metaphorical "Rosetta stone" that will allow others to advance the science of flapping wing flight.

2.2 Wing Designs

2.2.1 Flapping Wings

The aerodynamics of flapping wings is characterized by unsteady aerodynamics. According to various researchers, flapping is divided into two stokes, downstroke and upstroke. During flapping, the vertical induced flow is maximum near the wing tips and its magnitude decreases towards the root. Thus for constant forwards speed, the relative angle of attack also decreases from the tip towards the root. To maintain low AOA at the tip the wing must pitch in the direction of the flapping, in order to maintain the attached flow. The forces generated by

flapping have been shown in Figure 2.1. During the downstroke, the total aerodynamic force is tilted forward and has two components, lift, and thrust. During upstroke, the AOA is always positive near the root but at the tip, it can be positive or negative depending on the amount of pitching up of the wings. Therefore, during upstroke, the inner part of the wing produces an aerodynamic force which is upwards but tilted backward producing lift and negative thrust. The outer region of the wings would produce positive lift and drag if the AOA is positive. But if AOA is negative then it will produce negative lift but a positive thrust.

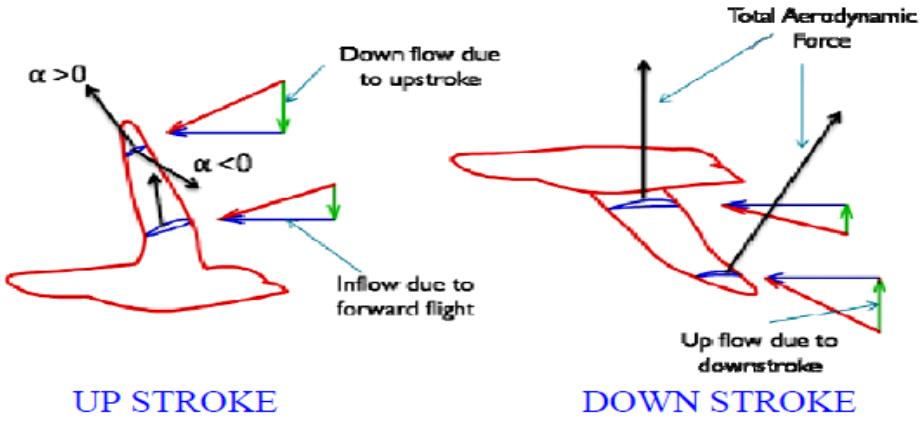

Figure 2.1 Forces generated during Flapping

Alphonse Penaud, in the 1870s performed a mechanical flapping wing rubber powered model ornithopter in France, which was documented and witnessed. Alexander Lippisch also worked on ornithopters. During the 1990s The Project Ornithopter engine powered piloted aircraft was which is based on the technology of the Harris DeLaurier model. One of the first successful attempts to develop bird-like flapping flight was by DeLaurier. The first MAVs were developed as early as WW-I in the form of guided munitions later expanding their roles into radio-controlled target drones, reconnaissance aircraft and glide bombs of the modern day cruise missile. The first radio-controlled (RC) aircraft flight in Germany 1936 led the way to further refinement of small UAVs in the post-war era. The air flow field in flapping wings cannot be assumed as steady. A large angle of attack would lead to flow separation and turbulence too. Obviously, there must be phenomena producing extra lift. As was discovered with the development of MEMS technology, the physics of the small is different from that of the large (for example, friction is more important than gravity). For MEMS technology to progress, researchers had to develop a new understanding of these physics, and develop new techniques for overcoming and capitalizing on them. This is the case with small scale, or low Re aerodynamics today. Flapping flight is more complicated than a flight with fixed wings but still, the basic concept of the aerodynamics of fixed wing can be applied. The thin membrane of flexible material can be stuck on the leading edge and root chord of the wing. The thin membrane is used for the wing is non-woven fiber and cellos plastic. According to the Ornithopter Design Manual (Chronister, 1996) and Micah O Halloran (1998), membrane wings generate positive lift and thrust during the down stroke. However, during the upstroke, the lift becomes negative although thrust is still positive. The material of the membrane is flexible. Hence during the downstroke, air is displaced downward and backward, causing the membrane to be pushed upward and forward. The direction of this force will produce lift and thrust. Although the front of the membrane is glued to the leading edge, the trailing end is allowed to swivel within the limits of the flexible material. This will cause the trailing edge to always lag behind the leading edge. As a result, the membrane will become positively cambered. From fixed-wing aerodynamics, the chamber shape will provide some additional lift as well. According to the Ornithopter Design Manual (Chronister, 1996) and Micah OHalloran (1998), membrane wings generate positive lift and thrust during the down stroke. However, during the upstroke, the lift becomes negative although thrust is still positive. The material of the membrane is flexible. Hence during the downstroke, as shown in the air is displaced downward and backward, causing the membrane to be pushed upward and forward. The direction of this force will produce lift and thrust. Although the front of the membrane is glued to the

leading edge, the trailing end is allowed to swivel within the limits of the flexible material. This will cause the trailing edge to always lag behind the leading edge. As a result, the membrane will become positively cambered. From fixed-wing aerodynamics, the camber shape will provide some additional lift as well. Throughout the whole flapping cycle, the net force will only be the thrust because the positive and negative lift cancels each other out. In order to obtain lift, the forces must be redirected by increasing the pitch of the wing. In ornithopters design, this is usually achieved using the tail. The tail is tilted slightly upwards and this will cause the wing to pitch up during flight.

2.2.2 Rotatory Wings (Rotors)

The Igor I. Sikorsky Human-Powered Helicopter Competition represents the third largest monetary prize in aviation history. The monumental feat requires a human to required power for flight is a strong function of the rotor diameter: the bigger the span the less power it takes. A massive span, however, typically requires a heavy structure. In 1977 Paul McCready's human-powered aircraft, the Gossamer Condor, broke tradition and solved this structural problem with an elaborate system of guy wires. This same design approach can be applied to a human-powered helicopter. Making such a structure as light as possible requires extensive testing and precise computational modeling. In addition, the extreme flexibility of the rotor requires a thorough understanding of non-linear aeroelasticity, which, fortunately, is precisely the specialty of our team, having designed and tested accurate computational algorithms on the Snowbird Human-Powered Ornithopter. The final design of the Atlas is a quad-rotor design similar to the most successful helicopters before, with each rotor 10 m in radius. Both the rotors and large but lightweight overall truss structure make extensive use of wire-bracing, resulting in a more optimal design. Atlas, therefore, has a substantial size advantage over the Gamera II, the current record holder. In fact, per pilot mass, the Atlas requires 25% less power for flight. In addition, the Atlas' pilot Todd has 15% more power output than any of Gamera's pilots.

WING DESIGN & SELECTION

3.1 Introduction

As mentioned in the previous chapters, the inspiration for this model has been drawn from nature. Nature has laws of its own that have given birth to the scientific laws that we now follow. But the creatures of the world tend to follow the laws of nature more than the laws of science and technology. So many components of nature are still oblivion to the understanding of mankind. Only recently did the researchers find a flicker of success in comprehending the flight of insects, one of the tiniest yet most complicated flying creatures. The complete study of insect flight mechanism is still under progress. As the motive of this project is to mimic the mechanism of a dragonfly, the wing design is also based entirely on the wings of a dragonfly. To understand the movement and the structure of the wing, it first needs to be understood that they abide by the law of nature; they maneuver according to the changes in nature. Dragonflies are known for their controllability and maneuverability which is obtained by the design of their extremely detailed wing structure. It took years and years of research to finally figure out the tiny parts of the dragonfly's wings. Each of these tiny parts plays a major role in giving it the flexibility and the rigidity it possesses. These wings are a pure work of art that blends in perfectly with the muscular movement of the dragonfly as it flies. A researcher and lecturer in bioengineering at Imperial College London, Dr. Huai-Ti Lin says, "Unlike an airplane wing, the dragonfly wing is a living structure with a neural network that is intricately integrated into the mechanical structure.

The conventional aircraft wing design is based on pre-computed aerodynamic models. It is very rigid, with little adaptability. These wings cannot deal efficiently with unpredictable air flow or extreme flight environments. Our bio-inspired approach will allow airplanes to cope with varied environments. This work will be particularly important for small aircraft and drones. It can also make wind turbines more efficient and flexible."

Dragonfly wings are not smooth surfaces but have distinct corrugations. The hind wing of a dragonfly is shown in Figure 3.1. These distinct corrugations define the stressed s0kin structure composed of girder-like veins and thin cuticle membrane.

Figure 3.1 Photography of the hind wing of a dragonfly

These complex geometries of the wing provide sophisticated mechanical advantages for resisting longitudinal bending while facilitating wing camber and torsion and enabling predictable, beneficial buckling, both within the normal wing stroke cycle and in response to sudden loads. Investigating the aerodynamic effect using physical and computational models of corrugations, it has been found that the incident flow separates at the ridges, enveloping recirculating eddies that might play a role in reducing skin friction drag or modulating the lift coefficient summarized in).

Three-dimensional models of insect wing corrugations have been limited to extrusions of chord profiles that are often based on a very limited set of measurements from a single wing of dried specimens, overlooking the consequences of span-wise variation in corrugation pattern, curvature of the ridges and valleys within the plane of the wing membrane, span-wise twist, three-dimensional aerodynamic effects, individual variation and interspecies diversity.

3.2 Parasite Force

Parasite power P_{par} is expended to overcome the parasite drag on the dragonfly body. The force required to overcome parasite drag D_{par} comes from the thrust generated by the wings, and thus parasite power is implicitly included in the induced power when this is derived from the total thrust. Studies of insect flight have traditionally divided the total thrust into vertical and horizontal components, which respectively balance the insect's weight and parasite drag. This is a convenient division because D_{par} is typically much smaller than the weight, and it can be estimated independently. Parasite power is then simply given by:

$$P_{Par} = VD_{par}$$

The overall thrust is nearly vertical, as required by the dominating role of weight support, so the induced velocity V is also approximately vertical. The induced power P_{ind} is conventionally calculated as if it is indeed vertical, and thus P_{ind} represents the kinetic energy imparted to the air solely for weight support. The kinetic energy imparted by the horizontal force component is ignored because it is treated independently by the D_{par} calculation, but it must be realized that the induced velocity has a horizontal as well as a vertical component. Where D_{par} is large, for

instance at fast flight speeds or where there are large horizontal accelerations, the induced velocity may differ significantly in magnitude and direction from the traditional estimate based on weight support alone. This will lead to errors, albeit probably small, in estimates of both the angles of incidence and the profile drag of the wings. Because of the accelerating flights in this study, the induced velocity was calculated from the total thrust; P_{par} is therefore implicitly included in P_{ind}.

3.2.1 Induced Power and Induced Velocity

To calculate induced power, the induced velocity resulting from total thrust production must first be calculated. Thrust is the vector sum of the weight support, the parasite drag, body lift and an unbalanced force that accelerates the dragonfly:

$$\mathbf{T = ma - mg - D_{par} - L_{par}}$$

Where; m is body mass, g is the acceleration due to gravity and a is acceleration. Preliminary calculations showed the lift generated by the dragonfly body, L_{par}, to be less than 1 % of the total thrust, and so it was ignored in the present study. This thrust implicitly includes the acceleration and drag components of the body, and so the induced power estimates also include the power required to accelerate the body and overcome parasite drag. To bring this thrust more in line with the weight support that is conventionally used for induced velocity calculations, the dragonfly coordinate system was transformed to a thrust-based X,Y, Z coordinate system where the thrust is vertical along the Z-axis, and the X axis is parallel to the sagittal plane (Figure 3.2). This thrust-based system is similar to the conventional gravitational coordinate system except that the 'vertical' force equals the thrust instead of the weight. The non-dimensional thrust $\hat{T}$ expresses total aerodynamic force as a proportion of the weight:

$$\hat{\boldsymbol{T}} = \frac{\boldsymbol{T}}{\boldsymbol{mg}}$$

Roll angles, which had reached 58 ° in the horizontal x', y', z' coordinates (Wakeling and Ellington, 1997), take values of less than 12 ° in thrust-based coordinates for all except one of the flights in the present study; these angles are more typical of results for insects flying at constant horizontal velocities in a wind tunnel. The actuator disc is, by definition, 'horizontal' in the thrust based coordinates.

It represents the area over which the wings interact with the air to give it a 'downwards' impulse and thus can be considered as the projection of the swept area of the wings onto the X,Y plane. This actuator disc is nearly parallel to the stroke plane, which is approximately normal to the thrust (see Wakeling and Ellington, 1997), so the actuator disc is taken to have an area $A_0=\Phi R^2$, where Φ is stroke amplitude and R is wing length. This estimation of actuator disc area is never more than 6 % greater than the equivalent areas $\Phi R^2\cos\beta$, where β is the stroke plane angle, used by Ellington (1984), Ennos (1989) and Dudley and Ellington (1990). The induced velocity was calculated from the mass flux of air that must be moved by the actuator disc to balance the thrust. The induced velocity w for the general case of a rotor with velocity V which is inclined at an angle $-\alpha'$ to the actuator disc is:

$$w^4 - 2Vw^3 sin\alpha' + V^2w^2 - \left[\frac{T}{2\rho A_0}\right]^2 = 0$$

It proves convenient to normalize this equation using the Rankine–Froude estimate of induced velocity w_0 required for hovering with $\boldsymbol{T=mg}$:

$$w_0 = \sqrt{\frac{mg}{2\rho A_0}}$$

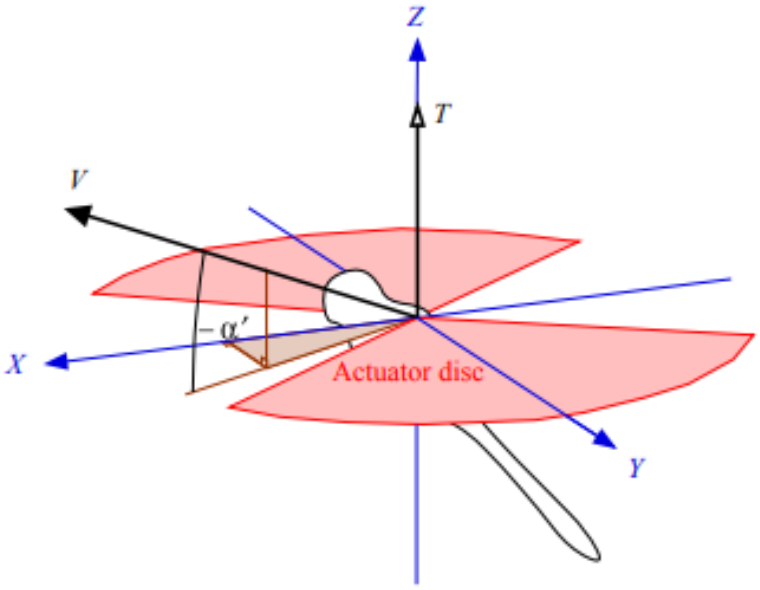

Figure 3.2 In the thrust-based coordinate system, the thrust *T* is 'vertical' along the Z-axis, and the dragonfly faces along the *X*-axis. The forward velocity *V* is inclined by – α' to the horizontal actuator disc in the *X, Y* plane.

3.3 Design Criteria

3.3.1 Bending and Torsional Stiffness

The corrugated structure of the dragonfly wing spars possesses great resistance to bending but is compliant in torsion and twisting of the leading or trailing edge results in torsion and relative movement of the remaining spars. As a result camber will automatically change and sets in the wing as it twists. In flight, the aerodynamic forces produced during the wing strokes will result in bending and twisting changing the camber that will help improve the aerodynamic efficiency. The bending and torsional stiffness values are determined for the dragonfly 3D model wing.

Bending stiffness

The bending stiffness '*Kb*' is the resistance of a member against bending deformation. It is a function of elastic modulus 'E', the area moment of inertia 'I' of the beam cross-section about the axis of interest, length of the beam and beam boundary condition. Bending stiffness of a structure can analytically be derived from the equation of structure deflection when it is applied by a force.

$$K_b = \frac{P}{W}$$

In the above equation 'P' stands for applied force and 'W' (W=δ) for deflection. Figure 3.3 shows the deflection of a cantilever beam when a load is applied on it.

Torsional stiffness

Torsional stiffness 'K_t ' is the measure of the amount of torque that a structure can sustain during its rotation in a mechanical system. The torsional stiffness of a structure can analytically be d
erived from the below equation.

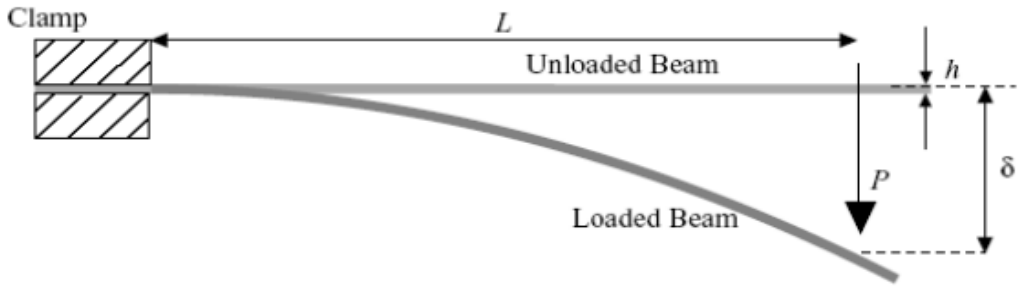

Figure 3.3 Bending of a cantilever beam

$$K_t = \frac{P}{\theta}$$

In the above equation 'P' stands for applied force and 'Θ' for angular deflection. In figure 3.4 the angular deflection of a cantilever beam is shown when a load P is applied on it.

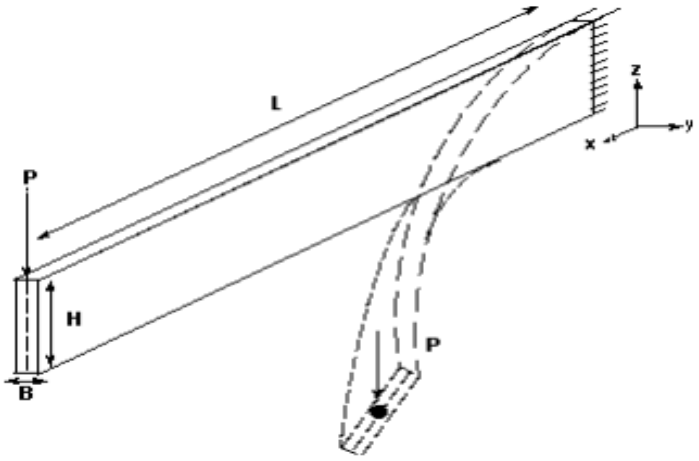

Figure 3.4 Torsion of Cantilever Beam

To summarize it all, dragonflies flap and pitch their wings at a rate of about 40 Hz, creating whirlwinds as illustrated in figure 3.5. As mentioned multiple times before, the peculiarity of the dragonfly is its use of a rowing motion along an inclined stroke plane. During hovering, the body lies almost horizontal. The wings push backward and downward, and at the end of the stroke, feather and slice upward and forward. In contrast, many other hovering insects use a symmetrical back-and-forth stroke near a horizontal stroke plane.

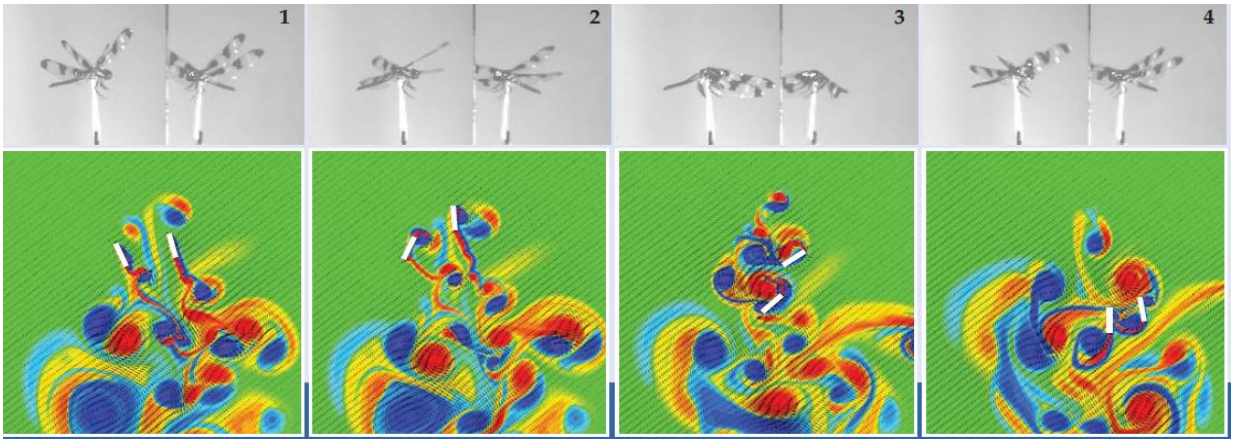

Figure 3.5 Stop-action dragonfly flight

The dragonfly's asymmetric rowing motion allows it to support much of its weight by the upward drag created during the downstroke; for the more common symmetric motion, the drag roughly cancels. Its fore and hind wings are controlled by separate muscles, and a distinctive feature of the dragonfly's wing movement is the phase relation between those wings during various maneuvers. When hovering, the fore and hind wings tend to beat out of phase; during takeoff, they tend to beat closer in phase. The dragonflies vary the phase in different maneuvers to alternate the downstroke reduces body oscillation. The fore and hind wings are about a wing-width apart—close enough for them to interact hydrodynamically.

To determine the amount of interaction, one solves the Navier–Stokes flow equations with boundary conditions set by the movement of the wings. The resulting flows are spectacular and complex. They depend on Reynolds number, wing motion, wing shape, and phase difference. Despite that complexity, two general results emerge: The aerodynamic power expended is reduced when the wings move out of phase, and the force is enhanced when the wings move in phase. When the fore and hind wings beat out of phase, they approach each other from opposite sides and cross near the midstroke. The fore wings experience an induced flow due to the hind wings, and vice versa. As a consequence, the drag on the wings is reduced, as is the power expended in flapping. But the reduction in drag on the two types of wing points in opposite directions, so the net force is essentially unaffected. In other words, the counter-stroking allows the dragonfly to generate nearly the same force while saving aerodynamic power. If instead, the fore and hind wings beat in phase, they will experience a higher drag due to the induced flow. In this case, the increase in drag on all the wings points is in the same direction. Thus the hydrodynamic interaction results in a greater net force that can be used to accelerate as needed during takeoff. The cost is greater power expenditure. Dragonfly wings are not entirely rigid. A close inspection of high-speed films such as the one used for figure 3.5 reveals a torsional wave that propagates from the wing tip to the root during pitch reversal. If the muscles were actively pitching the wing, one would expect the wave to propagate in the opposite direction, starting from the root where the muscles act. The observed tip-to-root direction suggests that aerodynamic force and wing inertia are responsible for pitching the wing. Indeed one can compute the aerodynamic torque and inertial force associated with the observed wing motions and confirm that they are sufficient to pitch the wing for dragonfly and other observed hovering wing motions. An insect can take advantage of the natural swinging motion

near the end of its wing stroke to simplify control and save energy. Thus, dragonflies wings opt for the wing structure and design of our human-powered flying ornithopter.

MATERIAL SELECTION

4.1 Introduction

The major challenge in Aviation Industry today to use components that would reduce the overall weight of the flying vehicle as much as possible and at the same time improves its strength and develops self-healing structures. When it comes to designing and fabricating a human-powered flying vehicle, it is extremely essential for the entire vehicle to weigh as low as possible but also be strong enough to bear the weight of a human pilot. Composite materials are mostly preferred for such cases. Composite materials are made from two or more constituting materials with extremely different physical and chemical properties, when combined together produce a material whose characteristics vary very much from the individual components. What sets apart composite materials from mixtures and solid solutions is the fact that the individual components remain separate and distinct within the finished structure. These materials are stronger, lighter and cheaper than their traditional counterparts. There are basically two main categories of constituent materials: matrix, which is also called the binder; and reinforcement. At least one portion of each type is mandatorily required to form a composite material. The matrix material surrounds and supports the reinforcement materials by maintaining their relative positions. The reinforcements impart their special mechanical and physical properties to improve the matrix properties. A synergism produces material properties inaccessible from the individual constituent materials, while the extensive variety of matrix and strengthening materials permits the designer of the product or structure to choose an optimum grouping. The matrix material can be introduced to the reinforcement before or after the reinforcement material is positioned into the mold cavity or onto the mold surface. The matrix material experiences a melding event, after which the part shape is essentially set. Depending upon the nature of the matrix material, this melding event can take place in various ways such as chemical polymerization for a thermoset polymer matrix, or solidification from the melted state for a thermoplastic polymer matrix composite. A variety of molding methods can be used according to the end-item design requirements. The principal factors impacting the methodology are the natures of the chosen matrix and reinforcement materials. Another important factor is the gross quantity of material to be produced. Large quantities can be used to justify high capital expenditures for rapid and automated manufacturing technology. Small production quantities are accommodated with lower capital expenditures but higher labor and tooling costs at a correspondingly slower rate.

4.1.1 Physical Properties of Composite Materials

The physical properties of composite materials are generally not independent of the direction of applied force, that is it is not isotropic in nature, but they are typically anisotropic (different depending on the direction of the applied force or load). The stiffness of a composite panel often depends upon the orientation of the applied forces and/or moments. The strength of a composite is bounded by two loading conditions as shown in the plot to the right. If both the fibers and matrix are aligned parallel to the loading direction, the deformation of both phases will be the same if it is assumed that there is no delamination at the fiber-matrix interface.

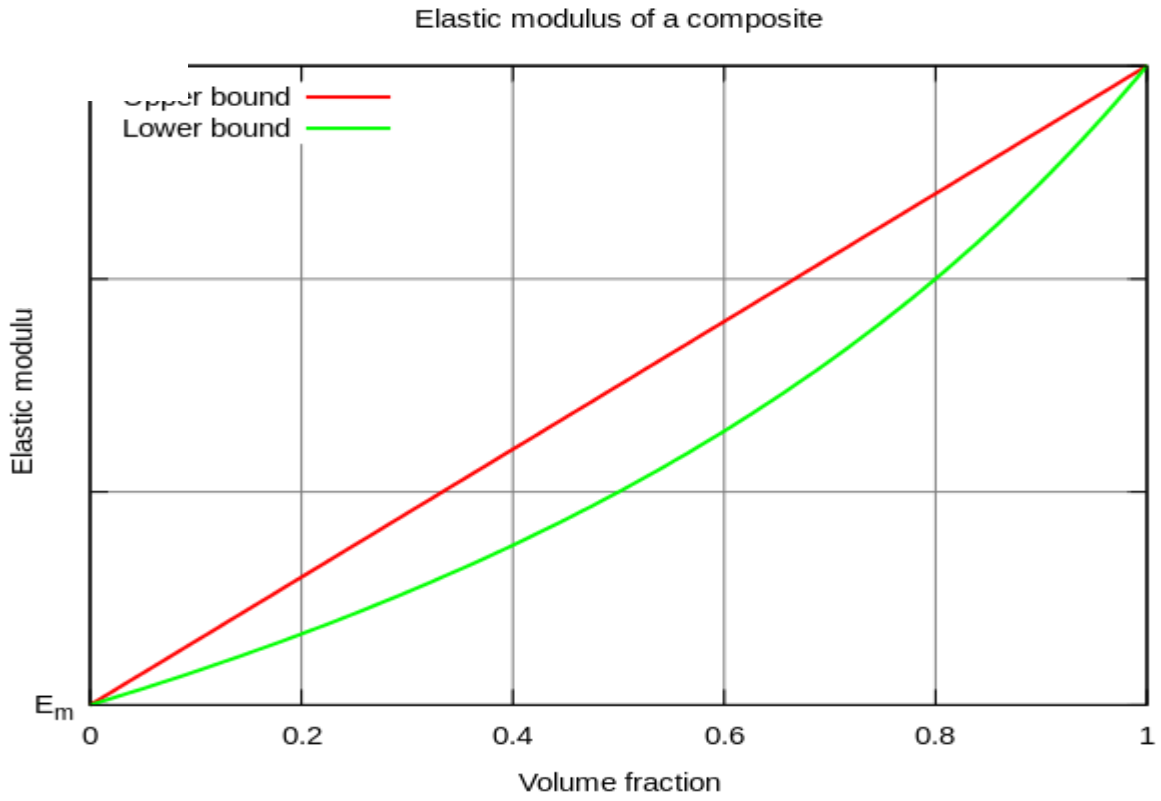

Figure 4.1 Plot of the overall strength of a composite material as a function of fiber volume limited by isostrain and isostress conditions.

This isostrain condition provides the upper bound for composite strength, and is determined by the rule of mixtures:

$$E_c = \sum_{i=1} V_i E_i$$

where E_C is the effective composite Young's modulus, and V_i and E_i are the volume fraction and Young's moduli, respectively, of the composite phases.

The isostrain condition implies that under an applied load, both phases experience the same strain but will feel different stress. Comparatively, under isostress conditions, both phases will feel the same stress but the strains will differ between each phase. Though composite stiffness is maximized when fibers are aligned with the loading direction, so is the possibility of fiber tensile fracture, assuming the tensile strength exceeds that of the matrix. When a fiber has some angle of misorientation θ, several fracture modes are possible. For small values of θ the stress required to initiate fracture is increased by a factor of $(\cos \theta)^{-2}$ due to the increased cross-sectional area ($A \cos \theta$) of the fibre and reduced force ($F/\cos \theta$) experienced by the fibre, leading to a composite tensile strength of $\sigma_{parallel}/\cos^2 \theta$ where $\sigma_{parallel}$ is the tensile strength of the composite with fibers aligned parallel with the applied force.

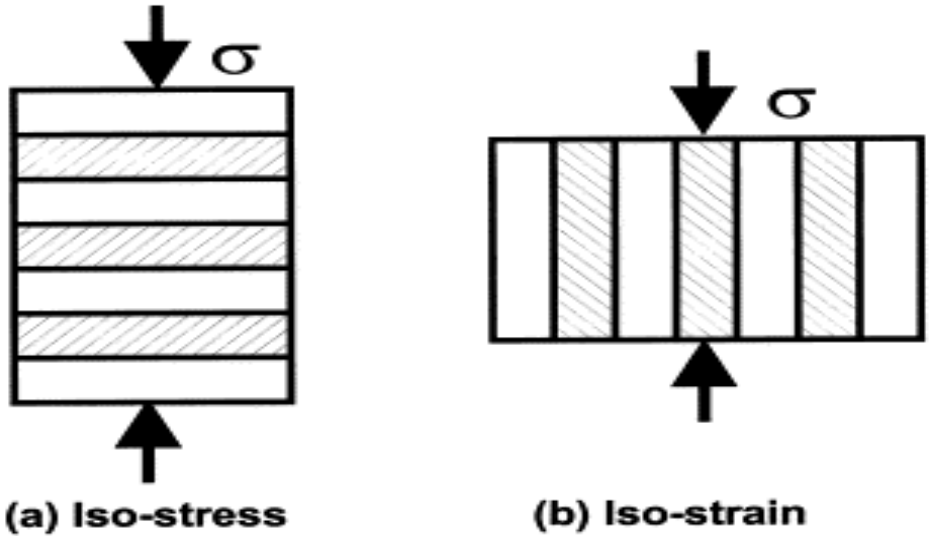

Figure 4.2 (a) Iso-stress- where the composite materials are perpendicular to the applied force.

(b) Iso-strain- where the composite materials are parallel to the applied force.

4.1.2 Modes of Failure in Composite Materials

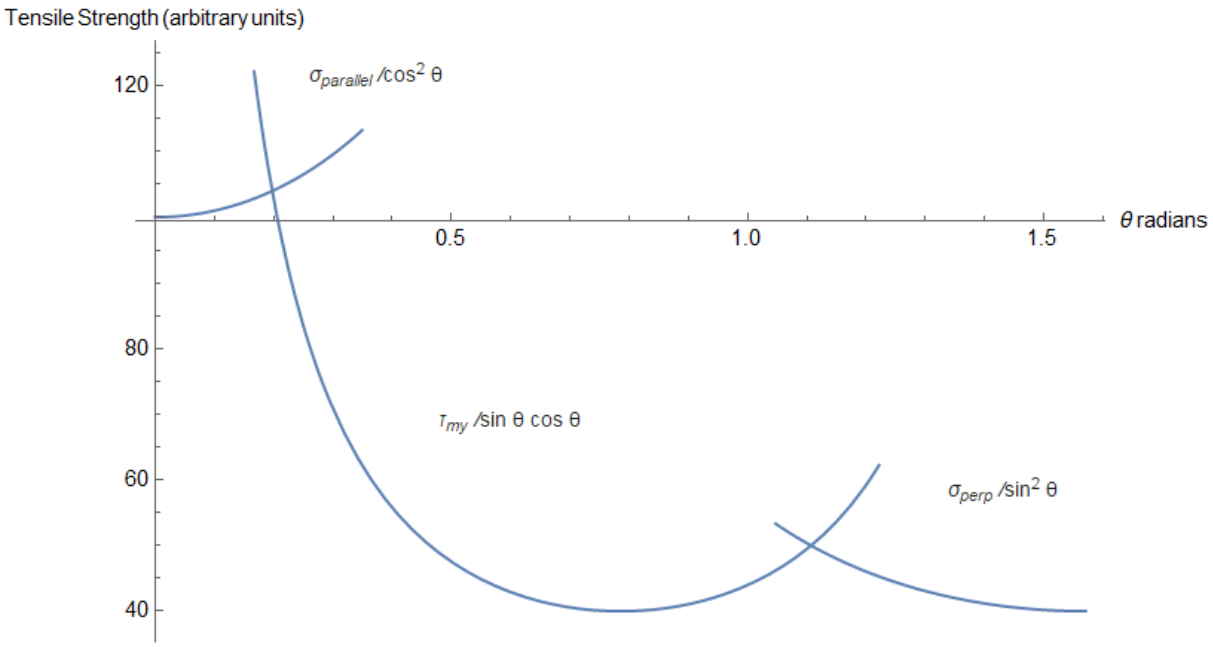

Figure 4.3 The graph depicts the three modes of fracture in a composite material.

Shock, impact, or repeated cyclic stresses cause the laminate to detach at the interface between two layers, this condition is known as delamination. Individual fibers can separate from the matrix. Composites tend to fail on the microscopic or macroscopic scale. Compression failures tend to occur at both the macro scale or at each individual reinforcing fiber in compression buckling. Tension failures can be net section failures of the part or degradation of the composite at a microscopic scale where one or more of the layers in the composite fail in the tension of the matrix or failure of the bond between the matrix and fibers.

Some composites are brittle and have little reserve strength beyond the initial onset of failure while others may have large deformations and have reserve energy absorbing capacity past the onset of damage. The variations in fibers and matrices that are available and the mixtures that can be made with blends leave a very broad range of properties that can be designed into a composite structure. Composites have relatively poor bearing strength compared to metals.

4.2 Materials to be used

4.2.1 Polystyrene Foam

Polystyrene foams contains 95-98% of air. They are extremely good thermal insulators. They also exhibit good damping properties and tend to provide high stiffness and rigidity with minimum weight. Thus these polystyrene foams will be used for the formation of the ribs and rims of the wings of our vehicle. Figure 4.6 shows the polystyrene foams of different sizes and thickness.

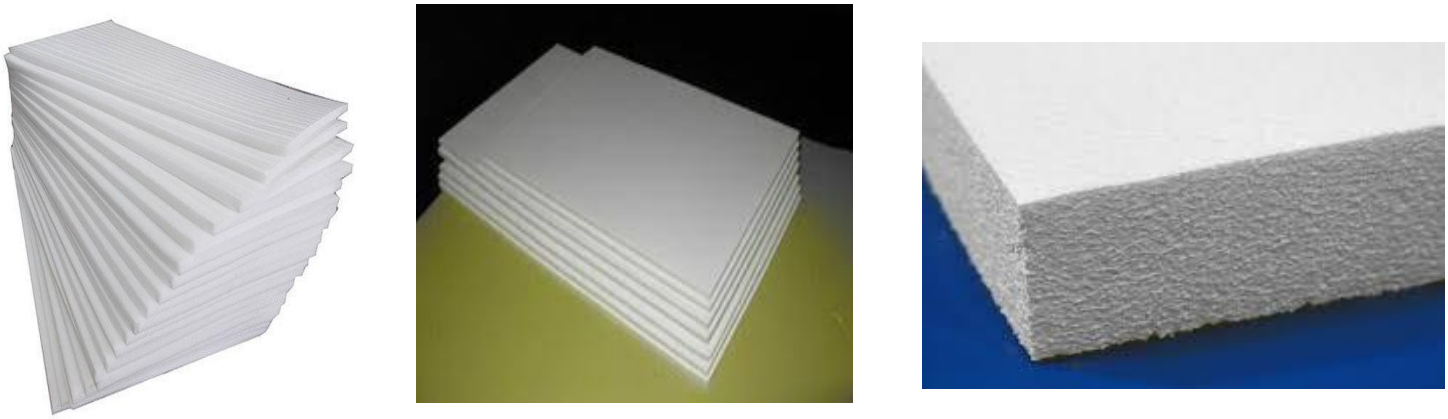

Figure 4.6 Polystyrene Foam

The wings have to be extremely flexible in order to flap in the required manner. The only stiff and rigid parts of the wings will be its rims and ribs but the overall weight of the wings need to be relatively low, thus polystyrene foam would prove to be an excellent manufacturing component.

4.2.2 Kelvar

Kevlar is by far the most known and the most commonly used composite material in the field of Aviation. Kevlar is heat resistant and strong synthetic fiber. It has tremendously high tensile-strength to weight ratio and by this measure, it is five times stronger than steel. Figure 4.7 show images of Kevlar sheets. Once it is spun, the resulting Kevlar fiber has a tensile strength of about 3,620 MPa and a relative density of 1.44. The polymer obtains its high strength to the many inter-chain bonds. These inter-molecular hydrogen bonds form between the carbonyl groups and N*H* centers. The additional strength is resultant from aromatic stacking interactions between adjacent strands. These interactions have a better influence on Kevlar than the van der Waals interactions and chain length

that typically influence the properties of other synthetic polymers and fibers such as Dyneema. The presence of salts and certain other impurities, especially calcium, could interfere with the strand interactions and care is taken to avoid inclusion in its production. Kevlar's structure consists of relatively rigid molecules which tend to form mostly planar sheet-like structures rather like silk protein. Kevlar will be used for the formation of the firm leading and trailing edge of the wings and pilot seats of our flying vehicle.

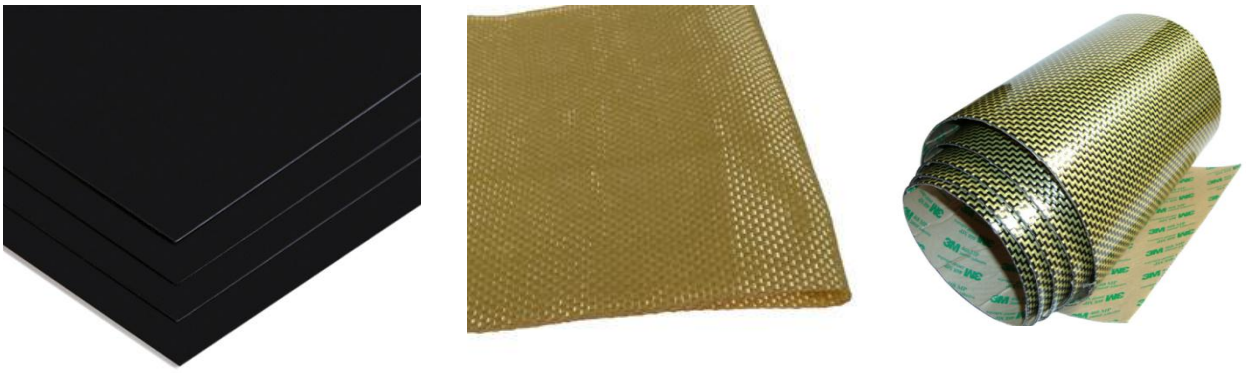

Figure 4.7 Kevlar

4.2.3 Carbon Fiber Tubes

Carbon Fiber Tubes are characterized by their extreme light weight and tremendous strength along with high stiffness, high tensile strength, low weight, high chemical resistance, high-temperature tolerance, and low thermal expansion. All of these properties make carbon fiber tubes apt for the formation of all the rod-shaped structures of the vehicle. Figure 4.8 shows the different shaped carbon fiber tubes.

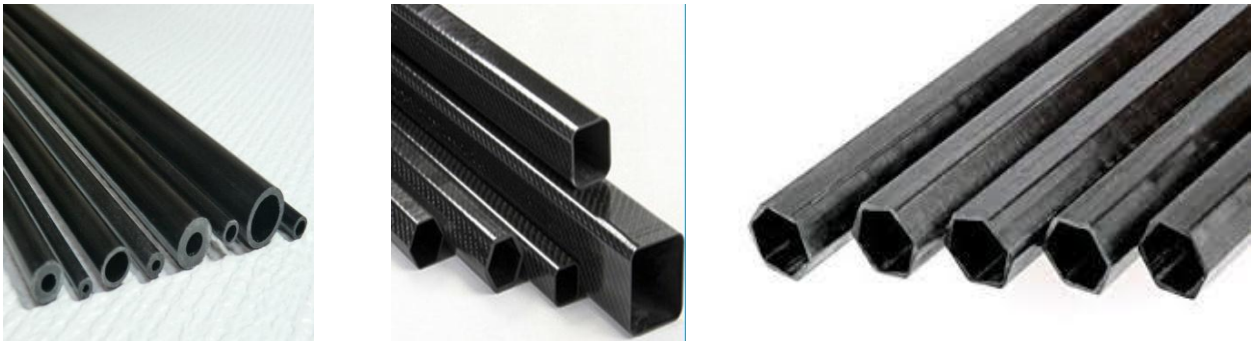

Figure 4.8 Carbon Fiber Tubes

4.2.4 Balsa Wood

Balsa Wood and Base Wood are lightweight; rigid and strong (Figure 4.9). This will be used for the formation of the main body of the flying vehicle.

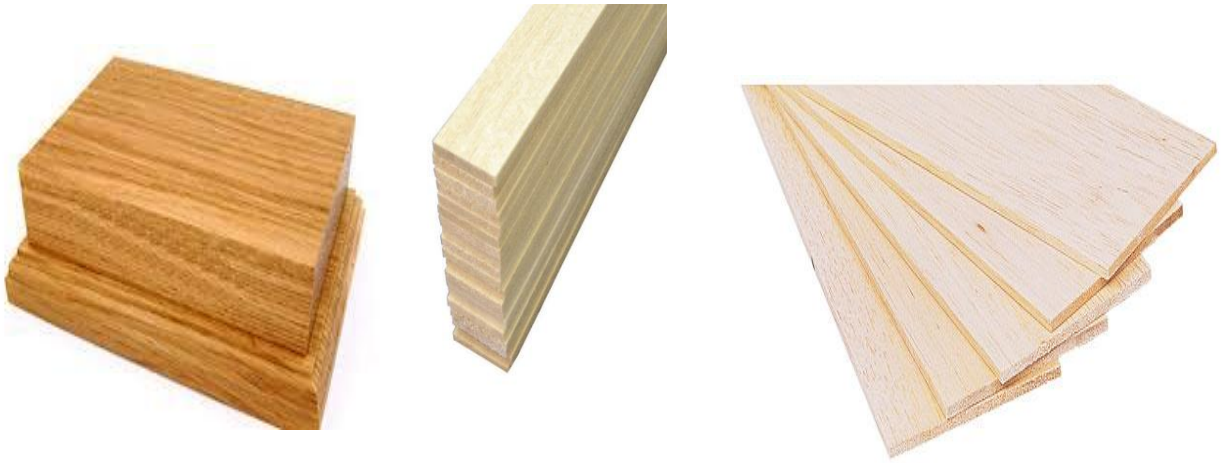

Figure 4.9 Balsa Wood

4.2.5 Mylar Film

Mylar Film is characterized for its properties of having high tensile strength, exceptionally low weight and transparent (Figure 4.10). Mylar film will be used for the skin of the fuselage and the wings. They are highly resistive to greater load and pressure, thus when the vehicle is in the air, this film would be a cover of protection for the pilot.

Figure 4.10 Mylar Film

FABRICATION PROCESS

The function of the flapping wing mechanism is to convert the rotatory motion into the flapping motion. Construction of the flapping wing mechanism is the most important task of this project. In the last few years, researchers have assessed many different aspect designs on the mechanism but they were all similar except for the slight modification. Simplicity is the key to this project. The most basic of the flapping wing design is the staggered crank. We designed the power transmission system of the human power to flap the wing through a staggered crank system which is design with a design with AUTOCAD and fabricate using the light materials such as polycarbonate tube for the prototype.

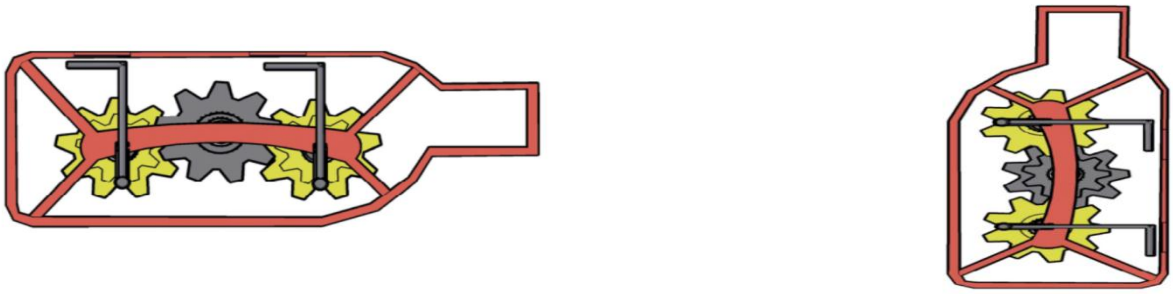

Figure 5.1 Staggered crank

The entire fuselage system required to be very light in compared to the lift generated to the wing, so the possible weight of the wing is around 1.5%-4% of the entire body mass. And the possible weight of the pilot is twice the empty weight of the aircraft.

A distinguishing feature of this is the use of hand cranks in addition to the more conventional foot cranks in the four wings flapping flight mechanism. In the earlier projects on human power flying vehicles, the 60-second target flight duration of Gamera II puts the human pilot in a very different regime, in a physiological sense, than other, longer duration human powered vehicles.

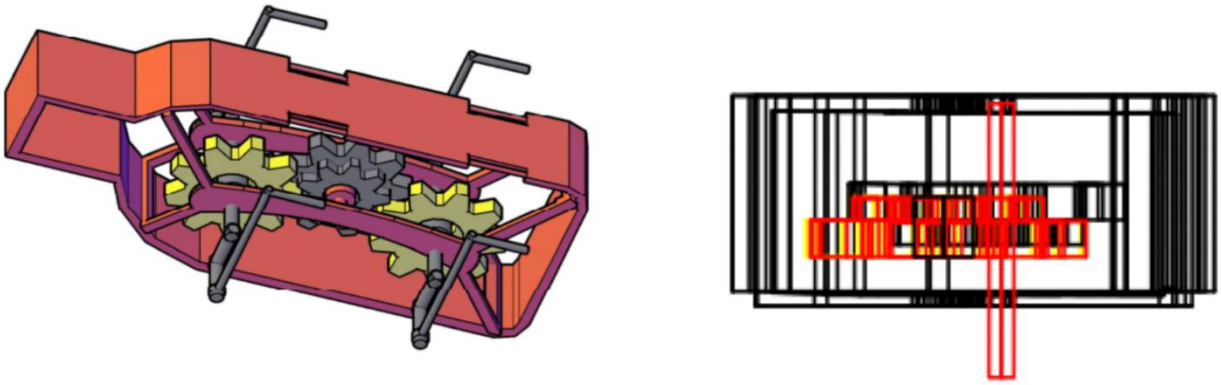

Figure 5.2 Gear transmission system

Exercise physiologists have estimated that for short-duration exercises, between 20 and 60 seconds, energy production is fueled almost entirely by anaerobic glycolysis. This process relies on the glycogen stores within the active muscles. The implication is that engaging more muscle mass should release more stored energy (glycogen). There were relatively few controlled experiments found in the literature comparing the short-duration power output of exercises with and without the additions of the upper body. Ursinus' experiments from 1936 are commonly cited in human power publications. Experiments were performed on one subject involving several mechanisms but notably compared leg cranking with leg and hand-cranking.

Figure 5.3 Recumbent seat for Pilot.

Wilkie shows that the addition of hand-cranking yielded about 30% more power output than cycling alone for a 60-second effort, with increasing gains at shorter durations. Evans concluded that for human-powered aircraft "useful improvements in the power-to-weight ratio may be obtained by the addition of arm work," estimating 50% more power for durations of 90 seconds.

Harrison conducted experiments comparing rowing (legs and arms) and cycling (legs only), also concluded that for the maximum power output of activities under 5 minutes the participant should make use of as much muscle mass as possible.

Despite this evidence pointing towards improvements in power with the addition of the upper body, it gave the team some concern that no other successful human-powered aircraft had employed hand cranks. The reasons for this absence on fixed-wing aircraft was fairly clear. For one, human-powered fixed-wing aircraft flight durations were measured from minutes (Gossamer Condor) to hours (Gossamer Albatross, Daedalus). These were well within the aerobic regime where engaging additional muscle mass has limited benefits.

More importantly, these pilots were pilots in the true sense; they required their hands-free to operate control levers in the cockpit. The previous two successful human-powered helicopters, the Da-Vinci III and the Yuri I, both utilized leg cranks only. There were no publications found to indicate whether those designers had considered adding hand cranks. Initial studies were done on hand cranking during the design of Gamera I, but an expanded testing effort was undertaken for Gamera II. Two of the test pilots, Colin Gore and Kyle Gluesenkamp, were systematically tested for power output on a commercial exercise machine that had both hand and foot cranks (Figure 2). For each test point, the pilot maintained a fixed RPM at a fixed resistance setting until exhaustion. Results are shown in a power vs. duration plot. Note that the horizontal axis is duration at constant power, not elapsed time. The results confirmed that the addition of hand cranks increases power output for the duration of interest. For the target flight time of 60 seconds, the addition of hand cranks can boost power output by about 20% to about 8.1 W/kg, or 500 W (0.67 hp) for a 61 kg (135 lb) pilot. The trends also indicate hand cranks offer a decreasing benefit as duration increases, which was expected from the physiology literature.

AERODYNAMIC LOAD MODEL

Calculation of the lift force is required to overcome the body weight. In this calculation, we neglected the loading of the wing due to the drag forces. Flapping flight lift is generated mainly by three distinct mechanisms: Delayed stall, rotational circulation, and wake capture. During the swing phases of the stroke, a leading edge vortex (LEX) is generated by the delayed stall. Rotational circulation and wake capture occur primarily during stroke reversal, while the LEV is a prominent mid-stroke. Because the total lift generated during the swing phase of the wing is typically considerably higher than the lift generated during stroke reversal, we focused on lift generated by delayed stall; the LEV.

The 'added mass' or 'virtual mass' is another aerodynamic load component which value varies from the 0.3 up to 1.2 times of the wing mass but it is difficult to model precisely and it is smaller than lift force, therefore we neglect it in our force model. Since an accurate estimate of both its magnitude and distribution over the wing is still unavailable for dragonflies, we neglected the drag forces.

List of symbols

AR	*Aspect ratio (l/c)*
C	*Chord length (m)*
CD	*Drag coefficient*
$CD_{,crit}$	*Drag coefficient at* α_{crit}
$CD_{,p}$	*Pressure drag coefficient*

$CD_{,f}$	*Friction drag coefficient*
$CD_{,I}$	*Induced drag coefficient*
$CD_{,min}$	*Minimum drag coefficient*
$CD_{,0}$	*Drag coefficient at* $\alpha = 0°$
CL	*Lift coefficient*
$CL_{,crit}$	*Lift coefficient at critical*
$CL_{,max}$	*Maximum lift coefficient*
$CL_{,0}$	*Lift coefficient* $\alpha = 0°$
CP	*Pressure coefficient*
D	*Drag (N)*
l	*Span length (m)*
l_{rel}	*Relative span length*
L	*Lift (N)*
p_0	*Measured pressure (Pa)*
p	*Static pressure of flow (Pa)*
r	*Radius of the leading edge (m)*
Re	*Reynolds number*
Re_{crit}	*Critical Reynolds number*
S	*Area of the profile (m2)*
S_c, D	*Standard error of CD (%)*
S_c, L	*Standard error of CL (%)*
U	*Velocity of the fluid (m/s)*
α	*Angle of attack (degrees)*
α_0	*Angle of attack (at* $C_L = 0$*) (degrees)*
α_{crit}	*Critical of attack (degrees)*
γ	*Gliding angle (degrees)*
εR	*gliding ratio (maximum range)*
ρ	*density of the fluid* (kgm^3)

We assumed that average lift generated by a forewing during a flap-cycle is equal to ¼ of the weight W of the dragonfly wing (because of its four wings) and equal during downstroke and upstroke:

$$L = \frac{1}{4}.W$$

Our aerodynamic load model is based on blade element theory:

$$\bar{L} = \frac{\rho_{air}}{2T} \iiint_0^{Trc} (\dot{\varphi}(t).x)^2.C_l(x)dydx$$

Here,

T = (1/f) is the period of one flap cycle,

ρ_{air} = the density of air at sea level (1.225 kg/m^3),

x= the spanwise distance from the root,

r= the wing length,

y= the position on the chord *c*, and

t= is time.

The angular velocity of the wing is:

$$\dot{\varphi}(t) = -\omega_{flap}.\Phi.\cos(\omega_{flap}t)$$

We distributed the lift over the wing chord spanwise with width dx, then speed and lift coefficient.

Then we distributed the spanwise lift distribution $C_l(x)$ chordwise using the chordwise pressure distribution:

$$C_l(x) = \int_0^c C_p\,(x,y)dy$$

Based on two second-order polynomials, the chordwise pressure coefficient was distributed. The first polynomial

$$P_1(y)=\alpha0+\alpha1\cdot y+\alpha2\cdot y^2$$

{which is defined from the leading edge (y_{LE} = 0) to the aerodynamic center (y_{ac})},

The second polynomial

$$P_2\,(y)=b_0+b_1\cdot y+b_2\cdot y^2$$

{From aerodynamic centre (y_{ac}) to the trailing edge (y_{TE} = *C*)}.

We assumed that the peak of the pressure distribution is to be at y_{ac} (at 1/4th of the chord length from the leading edge). Therefore pressure difference distribution can be calculated via:

$$\Delta P(x,y) = \frac{\rho_{air}}{2}(\omega(t).x)^2.C_p(x,y)$$

With this calculation, we can obtain a double curved pressure distribution over the wing area, which depends on the local pressure coefficient, angular velocity, spanwise position and time.

6.1 Pressure Measurements

Pressure measurements (*N*=3) were made with a micro pressure gauge and profile 4. The pressure values P_0 can be obtained by calculating as dimensionless coefficients of pressure C_P:

$$C_P = (p_0 - p\infty)/0.5\rho U^2$$

where p_0 is the measured static pressure of profile, $p\infty$ is the static pressure of flow and $0.5\rho U^2$ is the dynamic pressure, for α=−10° to +10° in 5° steps and U=1.74ms^{-1} (Re=9300).

6.2 Inertial Load Model

Accelerating wing mass can cause inertial load, Considering accelerations due to stroke and neglected accelerations due to the angle of attack changes. The inertial loads due to stroke can be calculated according to:

$$F(x,t) = \dot{\varphi}(t).x.(\frac{dm}{dx})dx$$

Based on a sinusoidal stroke, this angular acceleration is modeled:

$$\ddot{\varphi}(t) = -{\omega_{flap}}^2.\Phi.\sin(\omega_{flap}t)$$

For our finite element method calculation, the local masses should be calculated for each element and multiplied the volumes of each beam and shell element with the cuticle density ρ_c. The accelerations due to wing stroke were calculated at the center of each element. Then to obtain inertial "pressure load" divide the inertial force by element area on each element.

6.2.1 Load Cases

We analyzed four load cases that occur during the upstroke and four that occur during the downstroke of the wing. The difference between the four upstroke and downstroke load cases is the orientation of the airfoil with respect to the loading, is significant, because this an insect airfoil is asymmetric.

The load cases were defined as follows;

(i) Maximum aerodynamic lift loading, which occurs at mid-stroke $\varphi = 0°$, this lift points upwards opposing gravity during the upstroke and down-stroke.
(ii) Maximum load due to inertia occurs in the horizontal plane at stroke reversal (at $\varphi = \pm 60°$) during supination and pronation.
(iii) At $\varphi = \pm 30°$ four combined aerodynamic and inertial load cases were studied during both acceleration and deceleration of the wing for the upstroke and down-stroke case.

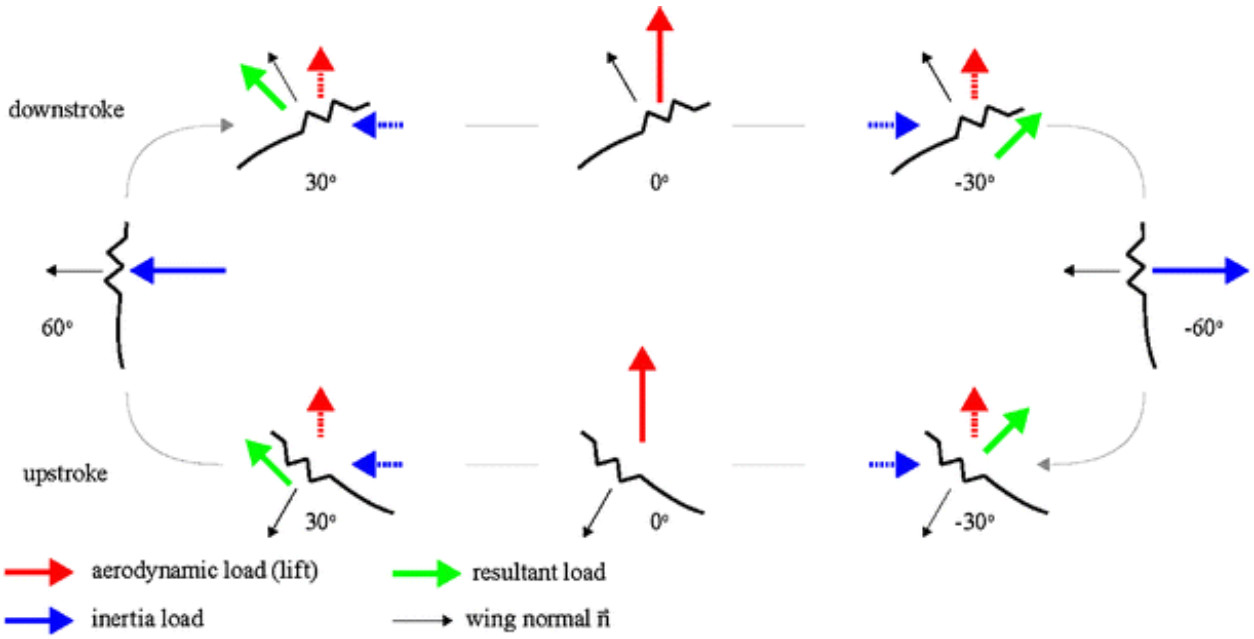

Figure 6.1: Load acting on the wing at a different angle.

The resulting load directions depend on the combination of the aerodynamic and inertial load, but the orientation of the airfoil depends on the flapping phase of down-stroke *vs.* upstroke.

Parameters		Dimensions	
Length		4.0 cm	4 x10^{-2}m
Mass		260 mg	2.60 x 10^{-4}kg
Wing Span	forewing	6.7 cm	6.7 x 10^{-2} m
	hindwing	6.5 cm	6.5 x 10^{-2}
Wing Area	forewing	4.42 cm^2	4.42 x $10^{-4}m^2$
	hindwing	5.44 cm^2	5.44 x $10^{-4}m^2$
Aspect ratio	forewing	10.2	
	hindwing	7.8	
Total wing loading		0.0264 gcm^{-2}	2.85 Nm^{-2}
The tilt angle of the wing roots		14^0	

Figure 6.2 Dimensions of the experimental Dragonfly.

Using the standard formulae:

$$C_L = L/(0.5\rho U^2 S),$$
$$C_D = D/(0.5\rho U^2 S),$$

where ρ is fluid density, U is fluid velocity and S is profile area, the dimensionless coefficients of lift C_L and drag C_D were calculated from the drag and lift forces. Total drag D is comprised of pressure drag plus induced drag plus friction drag.

The same is true for the drag coefficients:

$$CD = CD,_p + CD,_f + CD,_i$$

where

$C_{D,p}$ = the pressure drag coefficient,

$C_{D,f}$ = the friction drag coefficient, and

$C_{D,i}$ = the induced drag coefficient.

Since the wing profiles were limited at their upper and lower ends by a wall, they can be interpreted as having infinite length.

This allows a two-dimensional aerodynamic analysis in which the induced drag can be neglected. Thus,

$$CD = CD,_p + CD,_f .$$

Since the pressure drag of a flat plate at an angle of attack α of 0° approaches zero in the subcritical Re range, total drag is then equivalent to frictional drag. This coefficient can be calculated using the Blasius equation for laminar boundary layers:

$$CD,_f = 2.66/Re0.5$$

(Schlichting, 1979). For Re=10000, the expected minimum C_D value for an ideal flat plate with profile thickness t of zero at perfect laminar flow is, therefore, $C_{D,min}$=$C_{D,f}$=0.0266. Due to irregularities in the boundary layer and because of t>0, the measured value of $C_{D,\ min}$ should be greater than this value. An approximation is given by Ellington (1984) for Re from 100 to 10000:

$$CD,_{min} = 4.8/Re^{0.5} .$$

The aerodynamic performance of a wing during gliding can be determined with C_L/C_D ratios. The gliding ratio ε_R,

$$\varepsilon_R = (C_L/C_D),$$

gives the maximum gliding distance per unit height. The gliding angle γ can be calculated from:

$$\gamma = \arctan(C_D/C_L)$$

The gliding ratio $\boldsymbol{\varepsilon_s}$ gives the minimum sinking rate and can be calculated from:

$$\varepsilon_S = (C_L^3/C_D^2).$$

The gliding ratios ε_R and ε_S can be determined by calculating the ratios C_L/C_D and C_L^3/C_D^2 for each angle of attack α. The maximum value represents ε_R and ε_S, respectively.

6.3 Pilot Selection

The metric used to compare pilots was specific power measured in W/kg of body mass. Rotor momentum theory was used to get a first-order estimate of what the ratio of pilot weight to vehicle weight should be for minimum pilot specific power required. These results in the following formula:

$$\frac{P}{W_P} = \frac{1}{W_p} = \frac{1}{w_p}\frac{(W_p + Wv)^{\frac{3}{2}}}{\sqrt{2\rho A}}$$

$$= \left(\frac{W_P}{W_V} + 1\right)^{\frac{3}{2}} \left(\frac{W_P}{W_V}\right)^{-1} \sqrt{\frac{W_V}{2\rho A}} = \frac{d\left(\frac{P}{W_p}\right)}{d\left(\frac{W_P}{W_V}\right)} = 0$$

$$\frac{W_P}{W_V} = 2$$

This shows that the weight of the pilot should have to be twice the empty weight of the aircraft.

THEORETICAL ANALYSIS

Assuming wing root is a universal joint located at the symmetrical plane (X, Z), and its element can be specified by the coordinate of the radius r and azimuth angle Ψ in a stroke plane which is tilted by γ wrt X-axis directed backward in the horizontal plane. To make an orthogonal Cartesian coordinate system(X,Y, Z) , the Y directed to the right in the horizontal plane and Z-axis directed vertically upward. A local coordinate system (x,y,z) is defined as follows. The x-axis or the feathering axis is outward along the aerodynamic centre or the wing chord line and its is assumed to be common for all. The y-axis directed in the inflow at the wing section which is in consideration. The z-axis is directed to make an orthogonal Cartesian coordinate system togather with otthe her two axes.

Then the transformation matrix can be given by:

Figure 7.1 Transformation matrix

	X	Y	z
X	$-sin\Psi cos\gamma$	$cos\Psi cos\Phi cos\gamma + sin\Phi sin\gamma$	$cos\Psi sin\Phi cos\gamma - cos\Phi sin\gamma$
Y	$-cos\Psi$	$-sin\Psi cos\Phi$	$-sin\Psi sin\Phi$
Z	$-sin\Psi sin\gamma$	$cos\Psi cos\Phi sin\gamma - sin\Phi scos\gamma$	$cos\Psi sin\Phi sin\gamma + cos\Phi cos\gamma$

In the calculation of the aerodynamic forces, the following assumptions are made:

(i) A quarter of the total force, T/2 is sustained evenly by the respective wings, where T is the mean thrust or the mean force generated by the pairs of wing respectively and it is because of the negligible parasite drag of the body which is balanced by the weight: $\bar{T} = \frac{W}{2} cos\gamma$.

(ii) The pitch angle is independent of the spanwise position x=r/R where R is the half of the wingspan.

(iii) The forewing and hindwing generated induced velocities are constant over and normal to the stroke planes and are determined by the momentum theory as

$$V_f = -\left(\frac{V}{2}\right) + \sqrt{\frac{T}{2\rho S_e} + \left(\frac{V}{2}\right)^2} \quad \text{{for forewing}}$$

$$V_h = -\left(V + C_{hf} v_f\right) + \sqrt{\frac{T}{2\rho S_e} + (V + C_{hf} v_f)^2/4} \quad \text{{for hindwing}}$$

Where S_e is the swept area by one pair of wings and C_{hf} is an interference co-efficient indicating the induced velocity of the fore pair on the hind pair.

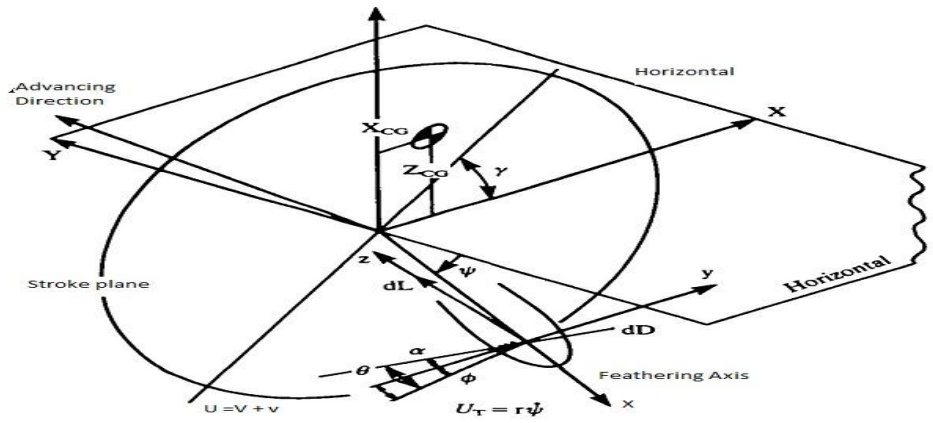

Figure 7.2 Co-ordinate system related to the beating motion of the wing.

The geometrical relationship about the wing stroke plane, the relative velocities and the aerodynamic forces of the wing for up and down –strokes respectively.

The perpendicular and tangential velocity components, U_T and U_p are given by:

$$U_T = r\Psi$$

$$U_p = V + v$$

Where,

$$\Psi = \Psi_0 + \Psi_1 \cos(\omega t + \partial_0)$$

$$\Psi = -\Psi_1 \omega \sin(\omega t + \partial_1)$$

Then the elemental drag and lift can be given by:

$$dL = \frac{1}{2}\rho U^2 c C_\lambda(\alpha) dr$$

$$dD = \frac{1}{2}\rho U^2 c C_d(\alpha) dr$$

Where,

$$U = \sqrt{{U_t}^2 + {U_p}^2}$$

$$U = \sqrt{(r\Psi)^2 + (V + v)^2}$$

$$\alpha = \theta - \phi$$

$$\phi = tan^{-1}(U_p / U_T)$$

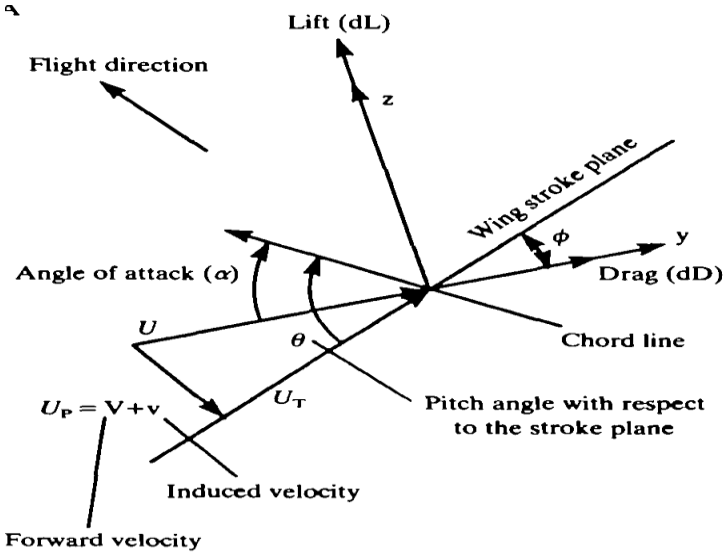

Figure 7.3 Force and directional vectors.

Since the drag and the lift of the wing element are directed towards the z-axis and the y-axis respectively. The total force generated by the one pairs of the wing along the X-axis and the Z-axes and torque Q, about the joint, can be written as follows respectively:

$$F_x = 2\int\{\mathrm{dD}(\cos\Psi\cos\phi\cos\gamma + \sin\phi\sin\gamma) + \mathrm{dL}(\cos\Psi\sin\phi\cos\gamma — \cos\phi\sin\gamma)\}$$

$$F_y = 2\int\{\mathrm{dD}(\cos\Psi\cos\phi\sin\gamma - \sin\phi\cos\gamma) + \mathrm{dL}(\cos\Psi\sin\phi\sin\gamma + \cos\phi\cos\gamma)\}$$

$$Q = 2\int\{dD\cos\phi + dL\sin\phi\}r.$$

Similarly,

The thrust is given by:

$$T = F_z cos\gamma - F_x sin\gamma = 2\int (dLcos\phi - \mathrm{dLsin}\phi)$$

$$= \rho \int_0^R V^2\, c\{C_\lambda cos\phi - C_d sin\phi\} dr$$

The heads-up pitching moment is given by:

$$M = F_z x_{CG} - F_x z_{CG}$$

$$= \rho \int_0^R U^2 c[x_{CG}\{C_d(\mathrm{cosCcos}\phi\mathrm{sin}\gamma - \ \mathrm{sin}\phi\mathrm{cos}\gamma) + C_\lambda(\mathrm{cos}\Psi\mathrm{sin}\phi\mathrm{sin}\gamma + \ \mathrm{cos}\phi\mathrm{cos}\gamma) - z_{CG}\{C_d(\mathrm{cos}\Psi\mathrm{cos}\phi\mathrm{cos}\gamma + \ \mathrm{sin}\phi\mathrm{sin}\gamma) + C_\lambda(\mathrm{cos}\Psi\mathrm{sin}\phi\mathrm{cos}\gamma — \ \mathrm{cos}\phi\mathrm{sin}\gamma)]dr$$

Required aerodynamic power is given by:

$$P = Q\Psi = 2\int (dLsin\phi + dDcos\phi) r\dot{\Psi}$$

$$= \rho \int_0^R U^2\, c\{C_\lambda sin\phi - C_d cos\phi\}\{-\Psi_1 \omega \mathrm{sin}(\omega t + \partial_1)\} r dr$$

Note: The aerodynamic power for feathering motion is neglected as being small.

CONCLUSION

As the successful flight of Gamera –I and Gamera-II has shown the possibility of a human-powered Vehicles. A team of three students from Excel Engineering College has designed a flapping wing mechanism mimicking the flight mechanism of the Dragonfly which is fully powered by the pilot's powered which is transmitted to the flapping wing through a special design staggered gear system which increases the flight endurance significantly. Construction of this project has been begun already. To able to maintain a long flight duration with the limited pilots powered, the weight of the aircraft is implemented using weight-saving technologies such as the dragonfly airfoil and recumbent seat and the specially design and develop of an efficient gear system for the flapping wing which reduced the weight of the aircraft.

A conceptual aspect of the aircraft shows the possibility of the flight to increase the hovering endurance and allow to shift the angle of attack to attain a stable flight path with multidirectional hovering accessibility. The use of the four flapping wings instead of the two wings will give more advantage to the lift and aerodynamic stability. Theoretical calculation of the aircraft shows the minimal weight of the aircraft will range from 26kg to 32kg with a

maximum flight endurance. Construction is underway and the various testing and fabrication process was doing a very hard pace.

ACKNOWLEDGMENT

This project would have been impossible to start without guidance, support, and mentor of the Prof. Dr.G. Manikandan and Asst. Professor Karthikeyan, Excel Engineering College. The team also would like to thanks Asst.Prof. Vivekananda who helps a lot to the insight of the fabrication process. This paper is solely dedicated to the team member of this project who made this conceptual into a reality.

REFERENCES

1. *Flight Mechanics of a dragonfly*. Institute of Interdisciplinary Research, Faculty of Engineering, The University of Tokyo, Tokyo, Japan.
2. *Design and Development of ATLAS Human-Powered Helicopter*. AeroVelo Inc. Toronto, ON, Canada
3. *Human Powered Helicopter: A program for Design and Construction,* Scott Alan Bruce, June. 1991
4. *Aspects of Flight Mechanics in Anisopterous Dragonflies,* A.C Neville, Zoology Department, Imperial College, London and Zoophysiological Department, University of Copenhagen, Denmark.
5. *Design Optimization of Gamera II: A Human-Powered Helicopter*. Alfred Gessow Rotorcraft Center, Department of Aerospace Engineering, University of Maryland, College Park.
6. Kesel, A. B., Philippi, U. and Nachtigall, W. (1998). *Biomechanical aspects of insect wings – an analysis using the finite element method*. Comp. Biol. Med. 28, 423–437.
7. M. Sun and J. H.Wu, *"Aerodynamic force generation and power requirements in forwarding flight in a fruit fly with modeled wing motion,"* Journal of Experimental Biology, vol. 206, pp. 3065–3083, 2003.
8. Dragonfly flight II. "*velocities, accelerations and kinematics of flapping flight,"* Journal of Experimental Biology, vol. 200, pp. 557–582, 1997
9. Jiyu Sun, Bharat Bhushan, *The structure and mechanical properties of dragonfly wings and their role on fly ability (2012)*
10. Adrian L. R. Thomas, Graham K. Taylor, Robert B. Srygley, Robert L. Nudds and Richard J. Bomphrey, *Dragonfly flight: free-flight and tethered flow visualizations reveal a diverse array of unsteady lift-generating mechanisms, controlled primarily via the angle of attack* (2004)
11. Javaan Chahl, Graham Dorrington, Sarah Premachandran, Akiko Mizutani, The Dragonfly Flight *Envelope and its Application to Micro UAV Research and Development*, IFAC Proceeding Volumes, Volume 46, 231-234 (2013)
12. C. DiLeo, *"Development of a tandem-wing flapping micro aerial vehicle prototype and experimental mechanism,"* Master's thesis, University of Delaware, 2007
13. M. H. Dickinson, F. O. Lehmann, and S. S. Sane, *"Wing rotation and the aerodynamic basis of insect flight,"* Science, vol. 284, no. 5422, pp. 1954–1960, 1999
14. *Structural Analysis of a Dragonfly Wings* Experimental Mechanics, Volume 50, Issue 9
15. *https://www.youtube.com/watch?v=tFPk1QqRixc;* Architecture of a Dragonfly Wing

16. *https://www.youtube.com/watch?v=cJJowVxiaRU;* Investigating the Secrets of a Dragonfly Wing
17. *https://www.youtube.com/watch?v=ZNdTt-ZNndA;* Dragonfly Vortex Formation during Flight.
18. *http://hpo.ornithopter.net/?q=content/the-project*
19. *https://www.youtube.com/watch?v=l008J4EhBFI*
20. *https://www.youtube.com/watch?v=ZAP2ucFsu7E*
21. *https://www.youtube.com/watch?v=d73wPF7SEnY*
22. *https://www.youtube.com/watch?v=P4rNX0gC*